This article should be cited as: Sharifzadeh M*, Wang L, Shah N, (2015). Integrated bio-refineries: CO_2 utilization for maximum biomass conversion. *Renewable and Sustainable Energy Reviews*, 47, 151–161, (Link).

Integrated biorefineries: CO_2 utilization for maximum biomass conversion

Mahdi Sharifzadeh[a*] , Lei Wang[b] and Nilay Shah[a]

[a] Centre for Process Systems Engineering (CPSE), Department of Chemical Engineering, Imperial College London. [b] Centre for Environmental Policy, Imperial College London.

Biomass-derived fuels can contribute to energy sustainability through diversifying energy supply and mitigating carbon emissions. However, the biomass chemistry p`oses an important challenge, i.e., the effective hydrogen to carbon ratio is significantly lower for biomass compared to petroleum, and biomass conversion technologies produce a large amount of carbon dioxide by-product. Therefore, CO_2 capture and utilization will be an indispensable element of future biorefineries. The present research explores the economic feasibility and environmental performance of utilizing CO_2 from biomass pyrolysis for biodiesel production via microalgae. The results suggest that it is possible to increase biomass to fuel conversion from 55% to 73%. In addition, if subsidies and fuel taxes are included in the economic analysis, the extra produced fuel can compensate the cost of CO_2 utilization, and is competitive with petroleum-derived fuels. Finally, the proposed integrated refinery shows promise as CO_2 in the flue gas is reduced from 45% of total input carbon to 6% with another 19% in biomass residue waste streams.

Key words: Energy sustainability, Integrated Biorefineries, Biomass Pyrolysis, Microalgae Cultivation, CO_2 Utilization, Technoeconomic Assessment, Life Cycle Analysis.

* Corresponding Author: Dr Mahdi Sharifzadeh; Room C603, Roderic Hill Building, South Kensington Campus, Imperial College London, UK. SW7 2AZ. E-mail: mahdi@imperial.ac.uk; Tel: +44(0)7517853422

1. Introduction

Motivated by scarcity of energy resources, and the pollutions associated with fossil fuels, significant research is devoted to exploring alternative renewable resources in addition to carbon capture and utilization [1]. Among other options, biomass-derived fuels can play an important role in diversifying energy supply and enhancing its security. In addition, from a 'well-to-wheel' life cycle perspective, greenhouse gas (GHG) emissions occurred in production and use of biomass-derived fuels can be partially offset by the biogenic carbon sequestered in the biomass [2]. While the conventional biofuels (*e.g.*, bioethanol) are produced from agricultural crops, with the disadvantage of competition with human food supply chains, recent research has widely focused on producing advanced biofuels [3] from lignocellulosic biomass [4], algae [5,6] and various wastes [7-10].

The conversion pathways include pyrolysis, hydrothermal liquefaction and gasification [11], among which pyrolysis is widely recognized as the cheapest route toward renewable liquid fuels [12-14]. Despite the economic incentives, our knowledge of the pyrolysis pathway is still relatively limited. For example, Mettler *et al*., [15] identified ten research challenges for biofuel production through biomass pyrolysis, with emphasize on understanding the reaction mechanism. Nevertheless, research into biomass pyrolysis is multi-disciplinary and multi-dimensional. The diverse array of these research activities include advanced analytical chemistry methods for bio-oil characterization [16-18], developing kinetic models for the pyrolysis reactions [19], computational fluid dynamic studies [20], design of new reactors [21], developing new heating methods such as microwave assisted pyrolysis [22-23], optimizing the bio-oil yield [24], developing various bio-oil upgrading methods [25], process intensification [26], techno-economic analysis [27, 28] and environmental assessment [29], in addition to enterprise-wide and supply chain optimization [30-32]. A recent review of the research into biomass fast pyrolysis is provided by Meier *et al*., [33].

Nevertheless, biofuel commercialization poses an important challenge; the ratio of hydrogen atoms available for combustion to carbon atoms, (H-2×O)/C, of biomass is significantly smaller than fossil fuels. For example, the effective hydrogen to carbon ratio for hybrid poplar ($C_{4.1916}$ $H_{6.0322}$ $O_{2.5828}$) is

as low as 0.207 [35]. By comparison the same value for Octane (a representative component of Gasoline) is 2.25. As a result, in order to convert biomass to liquid fuels, compatible with current energy infrastructure, all the oxygen atoms and a large portion of carbon atoms should be removed as carbon dioxide which deteriorates economic competitiveness of the biomass conversion processes. Therefore, CO_2 utilization is crucial for profitability of future biorefineries.

Several important integration schemes have been proposed by various researchers; an important strategy is to design for hybrid feedstock processes [36]. Examples of hybrid feedstock processes are co-processing coal and biomass [37, 38], and co-processing biomass and natural gas [39]. The important features of hybrid feedstock processes include improving the carbon conversion by adjusting the feedstock ratio and flexibility against fluctuations in the energy market. Similarly, integrating bioprocesses to existing petroleum infrastructures has gained researchers' interests [40, 41]. In parallel, other researchers [42, 43] proposed cogeneration of fuels and chemicals. While producing biofuel requires a high degree of deoxygenation, the application of biomass for producing chemicals may potentially skip costly oxidative processes and provide viable pathways toward production of alcohols, carboxylic acids, and esters [44, 45]. While these integrated biorefineries benefit from economies of scale and diversity of bioresources, they also face a challenge with respect to imbalanced product markets. This is because the chemical market is only approximately 5% of the fuel market.

In addition to the above-mentioned biorefineries with their advantages and limitations, a new class of integrated biorefineries should be proposed, based on carbon dioxide capture and utilization. The options for carbon capture vary from solvent-based technologies such as Absorption/desorption using Monoethanolamine (MEA) [46, 47], to underdeveloped methods such as oxyfuel combustion [48], membrane separation [49, 50], nanomaterial sorbents [51] and chemical looping [52, 53]. In parallel, intensive research is devoted to CO_2 utilization for producing fuel and products [54], and among them microalgae cultivation has gained significant research interest [55, 56]. The diverse array of the algae research activities includes microalgae strain selection and lipid yield enhancement, [57-58] microalgae cultivation and dewatering [59], oil-extraction and different upgrading methods [60-67], in

addition to anaerobic digestion of the lipid extracted algae [68], nutrient recovery [69] and biosorption of metals using algae biomass [70]. For a comprehensive review of microalgae technologies, the interested reader may refer to [71-73].

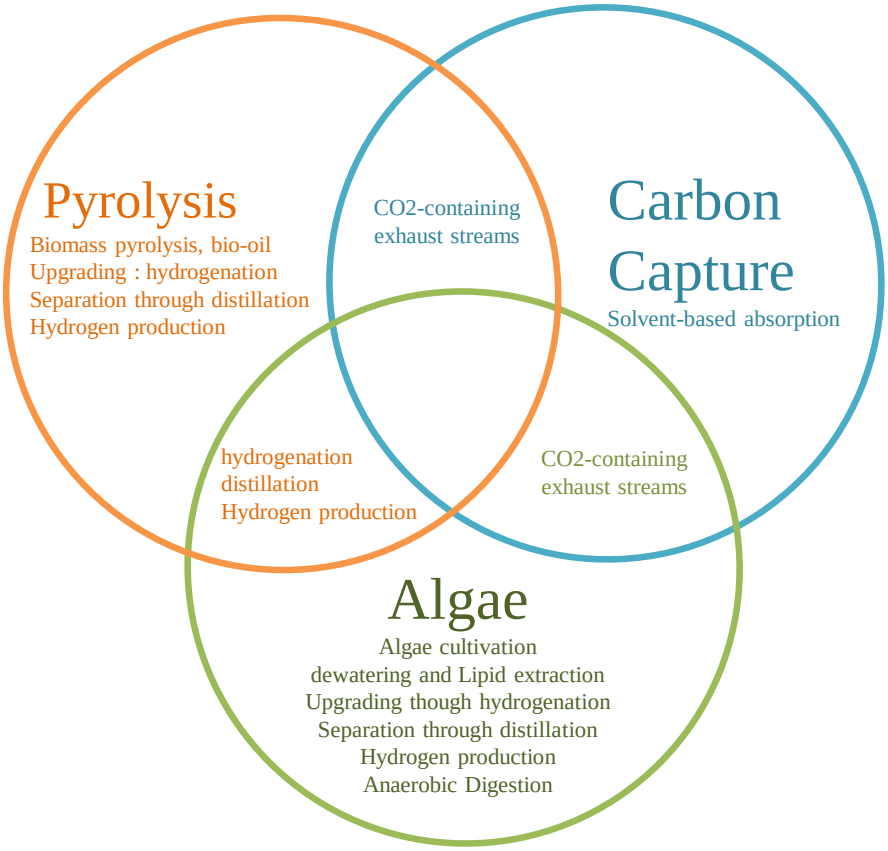

Fig. 1. Integrated refineries based on biomass pyrolysis and featuring CO_2 utilization through microalgae production

With the aim of enhancing the overall biofuel yields and improving the environmental impacts, the present research proposes an integrated biorefinery comprising of biomass pyrolysis, in addition to solvent-based carbon capture and utilization through microalgae cultivation. The process integration is based on the synergies between the processing steps of these processes, as shown in Fig. 1, and discussed later. It is also notable that the abovementioned combination (pyrolysis/solvent-based carbon capture/microalgae cultivation) is not unique. Other combinations of biomass conversion technologies (pyrolysis, gasification, torrefaction, fermentation, etc.) where considerable amount of high concentration CO_2 is available and can be exploited by a carbon capture technology (solvent-based, adsorption, membrane, chemical looping, etc.) and utilized for biofuel (algae cultivation) or

biochemical (e.g., urea) production can potentially fall into the proposed class of integrated biorefineries. Here the rationale behind process integration is synergies between the involved sub-processes in terms of sharing processing steps (e.g., hydrogenation for upgrading, anaerobic digestion for waste treatment and biogas production) and the cost-efficiency of carbon capture and utilization. With the present demonstrating case study, we aim at encouraging future research into process integration and CO_2 utilization among biorefineries.

While the proposed notion of integrated biorefineries featuring CO_2 utilization will benefit from the advancements in all the above-mentioned research directions, the present research will apply the already established base-lines (discussed later) from literature in order underpin the economic and environmental implications of the proposed integration scheme. In the subsequent sections in order to identify the incentives for process integration, firstly, the process description of each sub-process is discussed. Then, the Method Section reports the approaches that were employed for process modelling, economic evaluation and life-cycle analysis. Later, the results of the studies are presented and discussed. The paper concludes with discussion of research achievements and identifying the key research frontiers.

2. Process description

The following text describes the pyrolysis, carbon capture and microalgae processes as they operate stand alone. This introduction initiates a proposal for integration of these processes based on synergies between them.

2.1. Biomass fast pyrolysis and bio-oil upgrading

This process consists of a high-temperature, low-residence time pyrolysis reactor, followed by fast quenching in order to supress undesired secondary reactions which otherwise would decrease the yield of the condensable product in favour of light gases and char. The pyrolysis condensates form a brownish mixture with some undesirable properties. It has a higher oxygen content and a lower energy content compared to petroleum-derived fuels. It is also highly acidic and is immiscible with petroleum-based fuels. Therefore, it is necessary to upgrade the pyrolysis oil by hydrogenation and cracking heavy residues in order to improve the hydrogen content and convert oxygenates.

Bio-oil upgrading consists of several subsections. In the first section, the crude bio-oil is stabilized through hydro-deoxygenation reactions. Then, the stabilized effluents undergo a sequence of separation processes where the water, light dissolved gases and the de-oxygenated fraction with similar properties to diesel and gasoline are separated from the heavy fraction. The final stage of the upgrading process involves hydro-cracking of the heavy fraction and separation of the products.

2.2. Carbon capture and storage (CCS)

In order to separate the carbon dioxide from the flue gases, it is firstly cooled and cleaned of any particulate in a water-wash tower and then fed to an absorption column. In this column, carbon dioxide is chemisorbed into a solvent (*e.g.*, Monoethanolamine-MEA). The cleaned flue gas is washed with water in the upper section of the absorption column in order to minimize the solvent loss. The rich solvent, loaded with the absorbed carbon dioxide, is sent to the desorption column where the carbon dioxide is stripped and separated as the overhead product. The lean solvent is recycled and reused in the first column. The absorption process is exothermic and the desorption process is endothermic. Therefore, the lean solvent needs to be cooled and the temperature of the rich solvent should be increased, providing a heat integration opportunity between these two process streams.

2.3. Producing biofuel using autotrophic microalgae

This process converts the carbon dioxide to biodiesel. The first section consists of photobioreactors (PBRs) or open ponds (OPs) where carbon dioxide is converted to microalgae using solar energy and nutrients. Then, the microalgae concentration in the reaction effluent is increased using mechanical methods such as settling, flocculation, and centrifugation. Microalgae consist of lipids, carbohydrates and protein, from which only lipids can be converted to biodiesel. In the next stage, the microalgae cells are disrupted by pressurized homogenization and then the lipids are extracted using a butanol solvent. The effluent mixture, *i.e.*, the extracted lipids and solvent, is then sent to a distillation column for recovery and recycling of the solvent. The crude oil from the bottom of the distillation column is then sent to a hydrogenation reactor where the oxygenated compounds (triglycerides) are converted to biodiesel and a small fraction of naphtha. The residues of solvent extraction comprising of remaining lipids, carbohydrates and protein are sent to the anaerobic digestion section where they are partially

converted to methane, carbon dioxide (biogas) and cell-mass (bacteria). The produced biogas is exploited in a combined heat and power cycle (CHP) in order to produce electricity and steams. The water from microalgae concentration and also lipids extraction stages, containing the demineralized nutrients, is recycled back to the algae cultivation section.

2.4. Incentives for process integration

There are various synergies and integration opportunities among the above-mentioned technologies:

- The carbon conversion efficiency of the stand-alone pyrolysis is relatively low, which should be attributed to the biomass chemistry and the large amount of carbon dioxide produced during pyrolysis and upgrading. By converting the emitted carbon dioxide to microalgae biodiesel, integration can improve the overall carbon yield significantly, *i.e.*, more carbon is fixed in the products.
- The pyrolysis and microalgae processes both need hydrogen to upgrade the intermediate crude oils. In addition, the upgraded effluents need distillation in order to produce the end-use products. This synergy suggests that their integration can benefit from economies of scale.
- Carbon dioxide is produced during the pyrolysis and upgrading processes. In addition, CO2 is produced during production and combustion of biogas in the anaerobic digestion section. The costs of collecting, capturing and recycling of the carbon dioxide are minimal for the proposed integrated refinery because during the day the flue gas can be directly injected to the microalgae bioreactors, and the costs of carbon capture, compression and storage are only incurred during the night, and there is no need for CO_2 transportation.

Based on these synergies, the present research proposes an integrated biorefinery that is shown in Figs. 2a and 2b and comprised of Section 100: biomass pyrolysis, Section 200 upgrading, Section 300: product separation, Section 400: CO2 capture, Section 500: hydrocracking, Section 600: Hydrogen Production, Section 700: microalgae cultivation, and Section 800: anaerobic Digestion (AD). The applied method for integrating these sections is explained in Section 3.2. The flow diagrams of these sub-processes, their process descriptions and the applied modelling assumptions are reported in Electronic Supplementary Material (ESM).

This article should be cited as: Sharifzadeh M*, Wang L, Shah N, (2015). Integrated bio-refineries: CO_2 utilization for maximum biomass conversion. *Renewable and Sustainable Energy Reviews*, 47, 151–161, (Link).

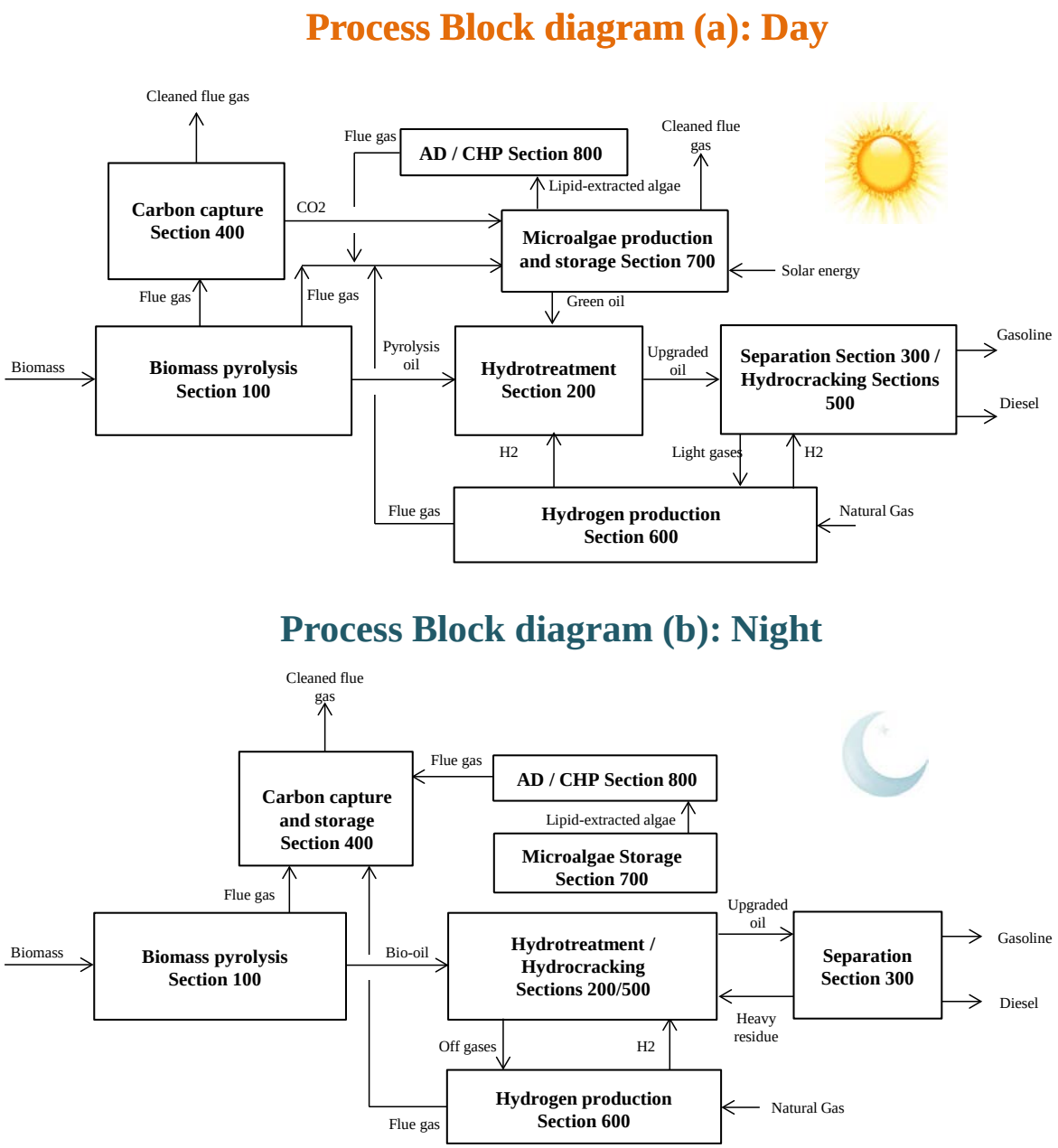

Figs. 2a, and b. The integrated biorefinery: day and night operational procedures.

3. Methods

The following sections report the research methodology. The features of interests include the choice of modelling baselines, seamless integration of the process sections, the assumptions regarding the economic evaluations, and the applied method for the environmental impact assessments.

3.1. Choice of modelling baselines

In order to develop reliable baselines for economic and environmental analysis, three established

studies were selected from literature and used as the starting points for the process modelling. The pyrolysis model was based on a study by US Department of Energy (DOE), conducted by Jones, *et al*. [74]. The microalgae model was based on studies by Davis, *et al*. [75] at National Renewable Energy Laboratory (NREL) and Frank, *et al*. [76] at Argonne National Laboratory (ANL). In addition, Process Systems Enterprise has published an example [77] of a rate-based model of the CO_2 capture process by MEA, which is validated based on experimental data [78]. This model was used as the starting point and was adapted to the process conditions. The process throughput was 2000 ton per day of biomass based on the DOE study. Accordingly, the algae process was scaled up to match this throughput. On this basis, the required land and water for the new scaled process is 4.24 larger than the NREL process for the Open Pond scenario and 6.29 times larger for the Photobioreactor scenario. These measures ensured that the modelling assumptions of those studies hold and the proposed biorefinery can be constructed in practice.

3.2. Seamless process integration

Figs. 2a and 2b show the day and night operations. As mentioned earlier, the process throughput was similar to Jones *et al*.,' study [74], *i.e.*, 2000 ton per day (tpd) hybrid poplar fed to the Pyrolysis Section 100 The Upgrading (200), Separation (300), Hydrocracking (500), Hydrogen Production (500), and Anaerobic Digestion (AD) sections operate 24 hours per day and their capacity is based on the pyrolysis section. However, since microalgae cultivation (Section 700) requires solar energy, it can only operate during daylight (assumed 12 hours per day on average). Therefore, for seamless process integration, the microalgae section (unit 700) should be sized at two times larger than the other processes. In addition, the carbon capture process operates only in the night-time. The produced CO_2 is captured, compressed and stored for the next day's operation. The CO_2 stored during the night is later consumed during the day. In addition, during the day operation, the flue gas is directly injected to the microalgae reactors (OP or PBR) in order to minimize the separation costs. Similarly, half of the produced lipids and lipid extracted microalgae are stored in the storage tanks during the day and fed to the corresponding processes during the next night. All the intermediate storage tanks were sized at five times the overall process capacity in order to ensure that malfunctioning of a section would not

interrupt the overall production for at least ten days. It was assumed that any produced steam is fed to the site steam headers and can be used in other parts. In addition, it was assumed that any extra electricity or steam produced can be exported and sold at the battery limit, at constant prices.

3.3. Economic evaluation

3.3.1. Cost estimation

It is assumed that this is the nth plant. This eliminates additional costs associated with pioneer plants by assuming other plants using the same technology are currently in operation. It is also assumed that 100% of the required investment is supplied from equity. The Total Capital Investment (TCI) is determined from to Total Purchased Equipment Cost (TPEC) and Total Installed Cost (TIC). The costs of process equipment are evaluated based on the developed process models. In the present study, the costs of conventional unit operations (*e.g.*, distillation columns, pumps, and vessels) were calculated using the Aspen Process Economic Analyzer™. However, the costs of the nonconventional unit operations (*e.g.*, catalytic reactors, pressure swing absorber) were calculated based on the following relation and with reference to the economic data from literature [74-77]:

$$\text{New cost} = \text{Base cost} * \left(\frac{\text{New size}}{\text{Base size}}\right)^{f_{scale}} \qquad (1)$$

A list of detailed equipment cost can be found in ESM. Once the TIC was determined, the indirect costs including engineering (32% of TPEC), construction (34%), project contingency (37%), legal and contractors' fees (23%) were added to yield the TCI. Land cost is $3000 per acre [75] for the algae cultivation section and 6% of the TPEC for the other sections. The variable operating costs including raw materials, utilities, and waste landfill charges are summarized in Table 1. The fixed operating costs including labour and maintenance and overheads as 95% of labour cost were scaled up based on Philipp, *et al.*'s study [84]. Maintenance and insurance were estimated to be 4% of the TCI.

Table 1. Summary of variable operating costs

Materials/Chemicals/ Utilities	Cost	Reference
Hybrid poplar	50.07 $/short ton	[74]
Natural gas	3.89 $/1000 scf	[81]
Hydrotreating catalyst	15.5 $/lb	[74]
Hydrocracking catalyst	15.5 $/lb	[74]
Hydrogen plant catalyst	15.5 $/lb	[74]
CCS solvent (MEA)	1.25 $/kg	[79]
DAP (algae cultivation nutrient)	0.44 $/lb	[75]
Ammonia (algae cultivation nutrient)	0.41$/lb	[75]
Butanol (algae extraction solvent)	0.94 $/lb	[75]
Fresh water	0.05 $/1000 gal	[75]
Disposal of ash	18.00 $/short ton	[74]
Waste water treatment	0.11 $/$m^3$	[80]
Electricity	37.02 $/MWh	[82]
Steam	0.003 $/kg	[83]
Fire heater	4.5 $/mmBtu	[83]
Cooling water	4.43×10^{-6} $/kg	[83]

3.3.2. Discounted cash flow method

Once the total capital investment and operating costs were determined, the minimum fuel selling price (MFSP) was calculated using a discounted cash flow analysis. The MFSP refers to the gasoline and diesel blendstock price at which the net present value of the project is zero at a set discounted rate of 10%. While two products are produced, (gasoline and diesel), they were combined and referred to as a 'biofuel product' for simplicity. The economic parameters used in the discounted cash flow calculation were adapted from [74]. The lifetime of plant is 20 years with 2.5 years as construction period and 6 months as start-up time. The income tax rate is 35% and the capital depreciation period is 7 years (MACRS method). The MFSP is reported as 2012 USD for cost distribution analysis and as 2007 USD for comparing with DOE's [74] and NREL's [75] recent studies.

3.3.3. Pump prices

In addition to comparison with the abovementioned baselines, this study also evaluated the economic competitiveness of the produced biofuel with the equivalent petroleum-derived fuels. The selected criteria was the biofuel price at pump, which was determined by including the production cost (MFSP), the fuel distribution cost (0.14 $/gallon [85]), sales tax (4% as general tax in the US [86]), fuel excise tax (0.244 $/gallon [87]) and subsidies (1.0 $/gallon [88]). The pump price of biofuel was

then compared with the petroleum-derived diesel retail price ($ 3.97/gallon in 2012) and gasoline retail price (3.68 $/gallon in 2012) [89].

3.4. Life Cycle Analysis for GHG emissions calculation

The Life cycle analysis (LCA) approach was applied to count GHG emissions for gasoline and diesel through their 'well-to-wheel' life cycles. The functional unit is defined as '1km travelled by a light-duty passenger vehicle'. The GHG emissions results are also reported for 1MJ of fuels produced to facilitate comparison with other LCAs. The machinery in hybrid poplar cultivation and the infrastructure in biofuel production were not included in the system boundary. The analysis of greenhouse gas emissions also included the waste streams from the pyrolysis and hydrotreating sections as listed in Table B.1. of [74]. The life cycle impacts of the biofuel production processes were allocated between gasoline and diesel on an energy-content basis (68.1% is allocated to diesel and 31.9 % is allocated to gasoline in PBR scenario whilst 64.4% is allocated to diesel and 35.6% is allocated to gasoline in OP scenario). The inventory data for poplar production were adopted from Gasol, *et al.*'s study (2009) and summarized in Table 2.

Table 2. Summary of inventory data for poplar cultivation [90]

Outputs (over 16 years)	
Poplar	216 o.d.t/ha
Inputs (over 16 years)	
Fertilizer (9N/18P/27K)	1800 kg/ha
Ammonium nitrate (33.5% N)	750 kg/ha
Stools	10000 stools/ha
Glyphosate (herbicide)	4 l/ha
Metil-pirimidos (insecticide)	1.5 l/ha
Propineb 70% (insecticide)	1 l/ha
Machinery	23.31 h/ha
Diesel consumption	345.4 l/ha

The mass balance including chemical utilisation and energy demand were obtained from an ASPEN Plus™ process simulation. The GHG emission factors for inputs in poplar cultivation, biofuel production processes and fuel storage as well as distribution were taken from the Ecoinvent database v2.2 (Table 3) [91]. Due to the lack of GHG emission factor for CoMo catalyst in hydrotreating and hydrocracking sections, data for zeolite was used as the surrogate [84]. Emission factors for

production and use of diesel as well as field emission factors of fertilizers were from IPCC, [92]. Assumptions about transportation are listed in Table 4. With regard to the utilisation of fuel in a passenger vehicle, 0.070 kg gasoline and 0.059 kg diesel are required to travel 1 km [93]. The GHG emissions occurr in vehicle operation when the passenger car travels 1 km, are 0.226 kg CO_2 eq. for gasoline and 0.190 kg CO_2 eq. for diesel [76]. The greenhouse gas emissions analysis also included the waste streams from the pyrolysis and hydrotreating sections [74]. The GHG emissions were derived from Ecoinvent database cooperated in Simparo™ software and were included in the LCA study.

Table 3. Summary of GHG emissions factors (EF)

	Production GHG EF in poplar cultivation, kg CO_2 eq./kg material	**Use GHG EF in poplar cultivation, kg CO_2 eq./kg material**		**GHG EF in biofuel production, kg CO_2 eq./kg material**
Diesel [a]	0.43	2.98	Natural gas	0.011 [c]
N fertilizer	9.12	0.011 [b]	Zeolite	2.90
P fertilizer	2.68	-	MEA	3.39
K fertilizer	0.8	-	DAP	2.76
Ammonia Nitrate	8.47	-	Ammonia	2.08
Glyphosate	10.2	-	Butanol	3.98
Insecticide unspecific	16.3	-	Electricity	0.48 [d]
			Steam	0.23
			Fire heater	0.07 [c]
			Ash to landfill	0.61
			Wastewater treatment	0.38 [e]

Note: [a] kg CO_2 eq./L; [b] Field emissions as N_2O are calculated based on IPCC method and reported as kg CO_2 eq./kg o.d.t poplar biomass; [c] kg CO_2 eq./MJ; [d] kg CO_2 eq./KWh; [e] kg CO_2 eq./m^3

Table 4. Assumptions about transportation

Materials	**Mode**	**Distance**
Fertilizers, insecticides, herbicide from wholesalers to farm	Diesel lorry 28 ton	500 km
Poplar chips from farm to bio-oil plant	Diesel lorry 16 ton	25 km
Chemicals from wholesalers to bio-oil plant	Diesel lorry 16 ton	50 km
Solid waste from bio-oil plant to landfill	Diesel lorry 16 ton	20 km

4. RESULTS

4.1. Mass and carbon balance

Figs. 3a-c show the results for the carbon yield distributions; these are based on 2000 ton per day (tpd) biomass feedstock. These results suggest that while the carbon conversion from biomass to biofuel products is limited to 55% in the pyrolysis stand-alone scenario, CO_2 utilization via the microalgae process increases the yield up to 72.9% and 67.6% for PBR and OP scenarios, respectively. Another important feature of interest is that while in the pyrolysis standalone scenario, 45% of the carbon is emitted to the environment, in the integrated scenario this measure is reduced to 6% and 19.3% for PBR and OP scenarios, respectively. In other words, for the integrated scenarios, more carbon is fixed in the products and most of the waste co-products are in the form of biomass residues and can be used as fertilizer or be landfilled.

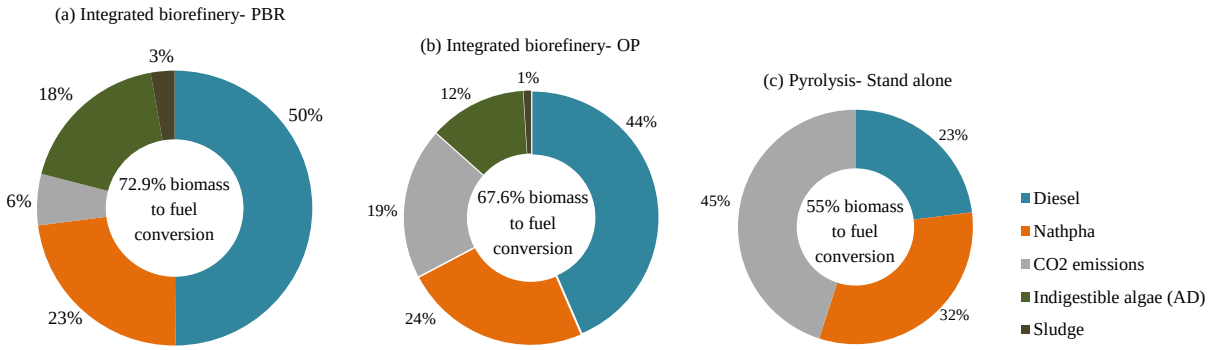

Fig. 3. Carbon yield distributions for (a and b): the present study (c): Jones *et al.*, [74]

4.2. Economic assessment

In order to compare the results of the present study with those in liteature [74, 75], the MFSP is recalculated backward to 2007 USD and represented in Fig. 4. The lowest benchmark is the result of Jones, *et al.*'s study [74] that reported the MFSP for gasoline and diesel blendstock to be 2.04 $/gallon for standalone pyrolysis scenario. The highest MFSP for diesel is found in Davis, *et al.*'s study [75] where diesel is produced by algae from CO_2 purchased from a nearby refinery using a photobioreactor system. They reported 20.53 $/gallon and 9.84 $/gallon (2007 USD) for the PBR and OP scenarios, respectively. The MFSPs in the present study are 6.64 $/gallon and 3.53 $/gallon (2007 USD) for the PBR and OP scenarios, respectively. The integrated biorefinery features a significantly better economic performance than the stand-alone algae-derived diesel plant. Please note that these results do not include the fuel tax and biofuel subsidies and are based on year 2007.

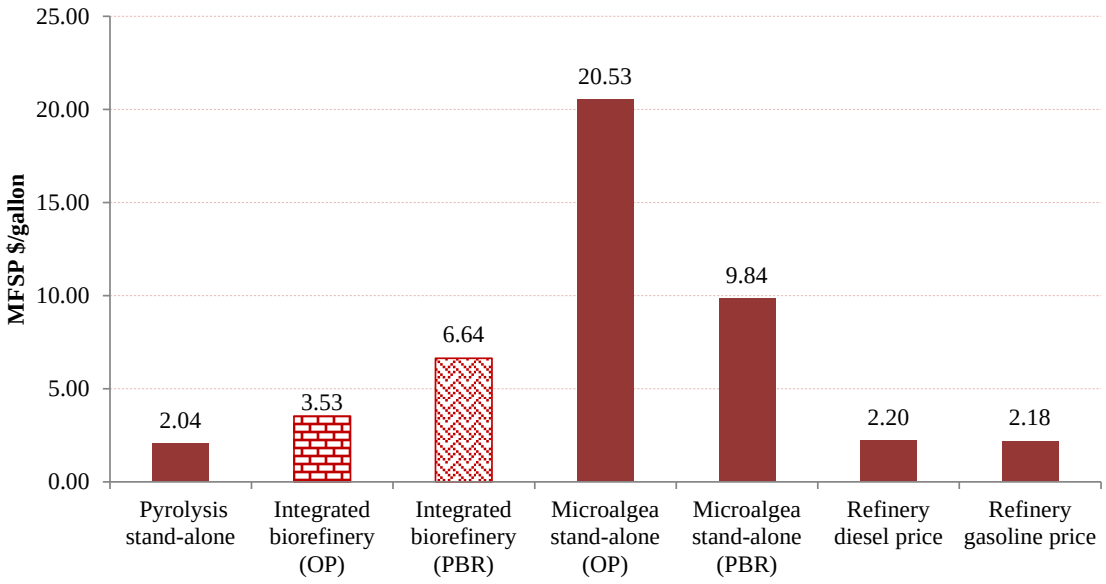

Fig. 4. Fuel cost in various studies compared with refinery diesel and gasoline prices at 2007. The Pyrolysis stand-alone scenario is the benchmark from Jones *et al.*, [74]. The Microalgae PBR and OP scenarios are the benchmarks from Davis *et al.*, [75].

The cost breakdown for the PBR and OP scenarios are shown in Figs. 5a and b, respectively. The resulting MFSP for diesel and gasoline blendstock are 7.33 $/gallon and 3.80 $/gallon (2012 USD), for PBR and OP scenarios respectively. In addition, in order to identify the key cost contributors, the detailed lists of equipment costs are reported in Tables S1 and S2 in the ESM. In both scenarios microalga cultivation, and hydrogen production are more costly than others. However, in the PBR scenario, the main capital cost contributor by far is photobioreactors which consist 68.1% of the total capital costs. For comparison this value is 8.9% for the open ponds. The contributions of each process section to the minimum fuel selling price (MFSP) are shown in Fig.s 6a and b. The microalgae cultivation Section 700, accounts for up to 67% of the MFSP in the PBR scenario. In this scenario, Hydrogen Production Section 600 is responsible for 12.5% of MFSP. By comparison, Sections 700 and 600 are responsible for 27.4% and 27.9% of MFSP in the OP scenario, respectively. In the PBR scenario the important raw material costs include: 43% hydrogen production, 24% pyrolysis and 24% algae nutrients and extracting solvent. Those values for the OP scenario are 45%, 25%, 21%, respectively. The algae cultivation and lipid extraction Section 700 accounts for 54% of the total electricity consumption in the PBR scenario. This large amount is needed for flocculation, centrifuge, homogenization and pumping the recycled water. This measure is even larger for the OP scenario (61%) due to more dilute effluents. The net electricity production of the combined heat and power cycle in Section 800 only addresses 3% and 5% of the PBR and OP scenarios, respectively. The reason is the high total electricity demand and low partial pressure of methane (67% on volumetric basis) in the biogas. While expansion of the stored CO_2 during the day offsets the required electricity demand for the CCS Section 400, the exergy loss results in the net loss of the available work and this section is a net consumer of electricity, *i.e.*, 15% for the PBR scenario and 11% for the OP scenario.

Another comparison (Fig. 7) can be made between the produced biodiesel and conventional fossil-derived diesel in terms of *pump price* which also includes the tax credits. In this case, the pump price of the biofuel (65% biodiesel and 35% biogasoline) in the OP scenario is 3.35 $/gallon which is cheaper than the petroleum-derived diesel (3.97 $/gallon in 2012) and gasoline (3.68 $/gallon in 2012) retail prices [89].

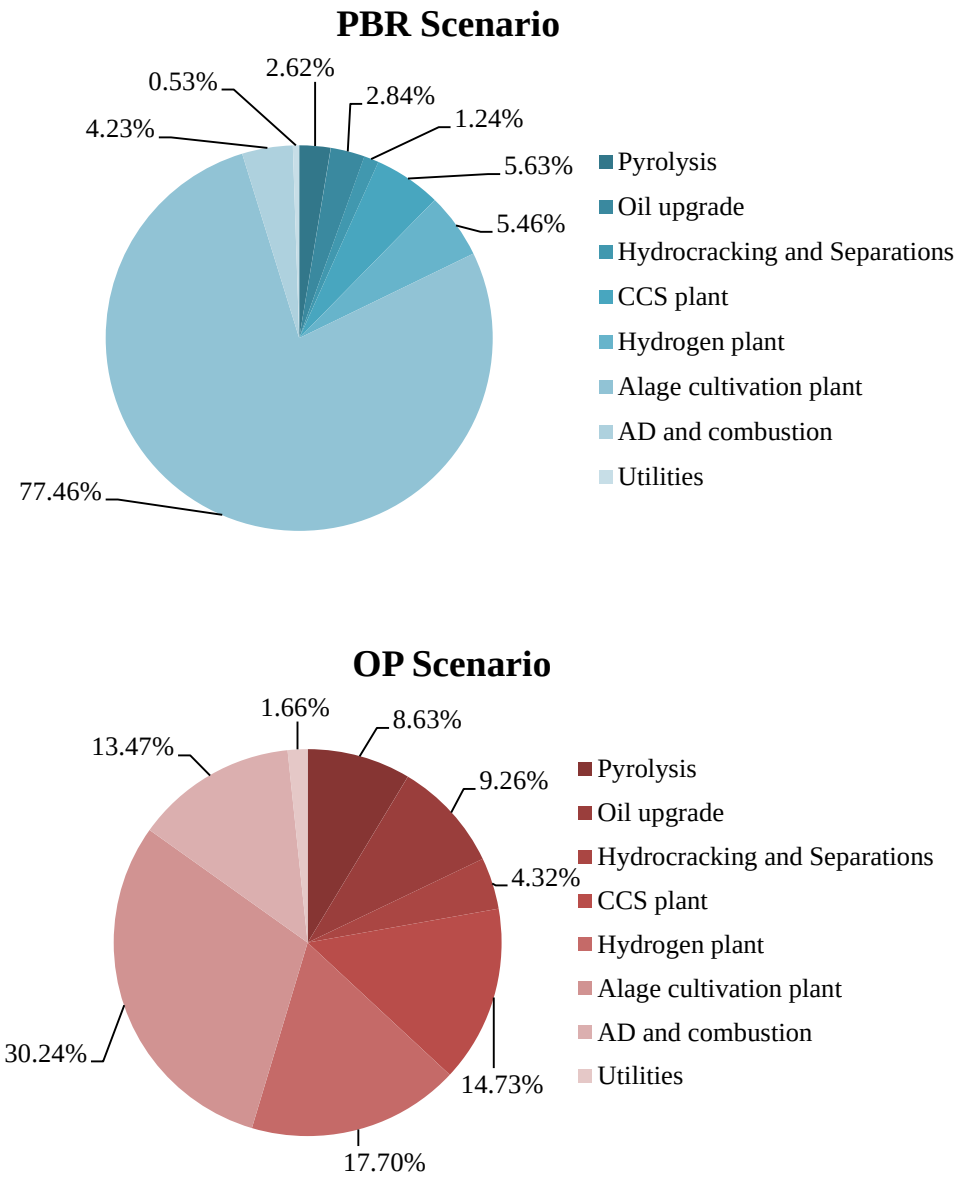

Fig. 5. The cost breakdown of MFSPs for gasoline and diesel blendstock: (a). photobioreactor scenario (b) open pond scenario.

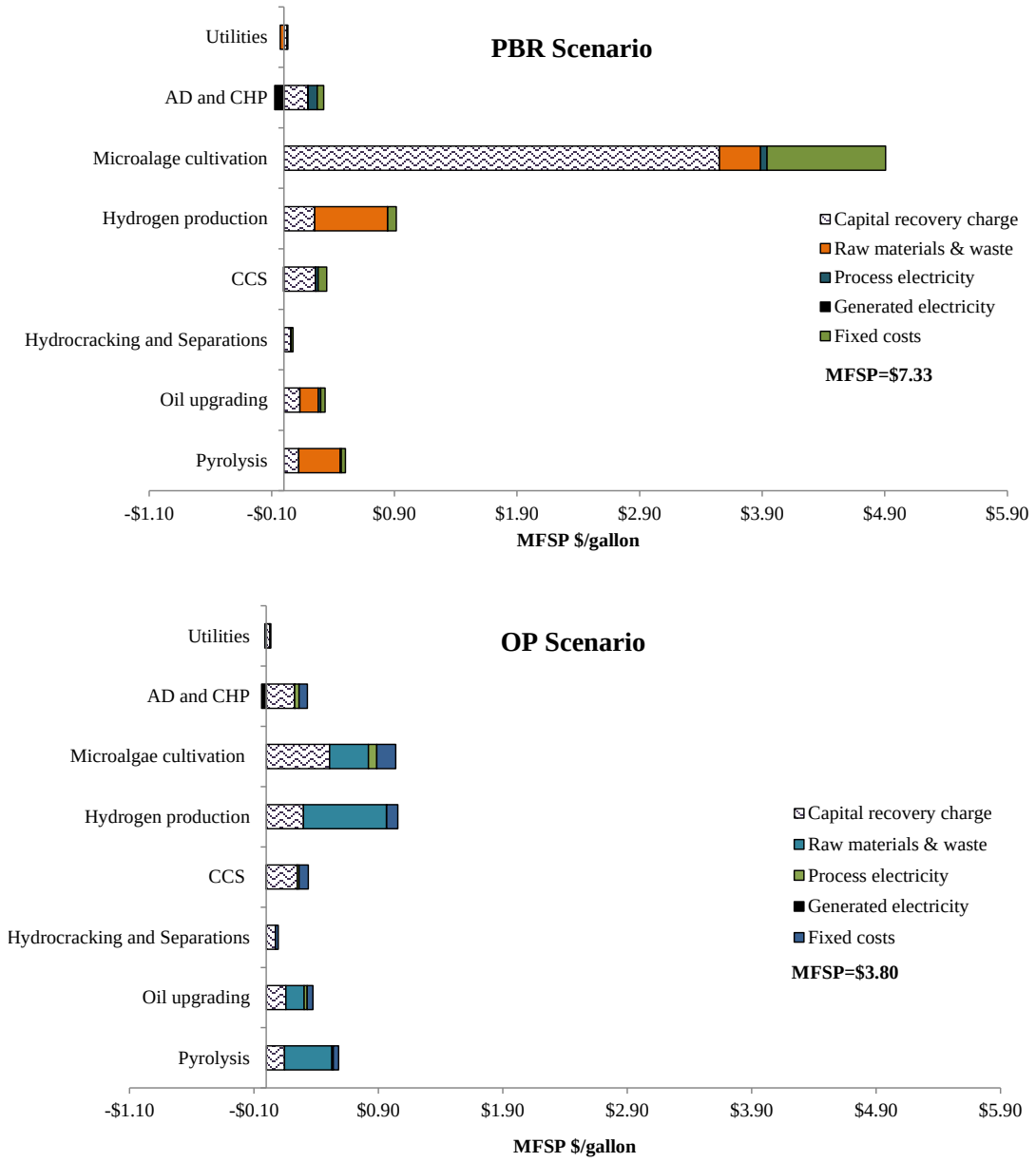

Fig. 6. The cost breakdown of MFSPs for gasoline and diesel blendstock for each section of the integrated bio refinery: (a) photobioreactor scenario (b) open pond scenario (2012-USD).

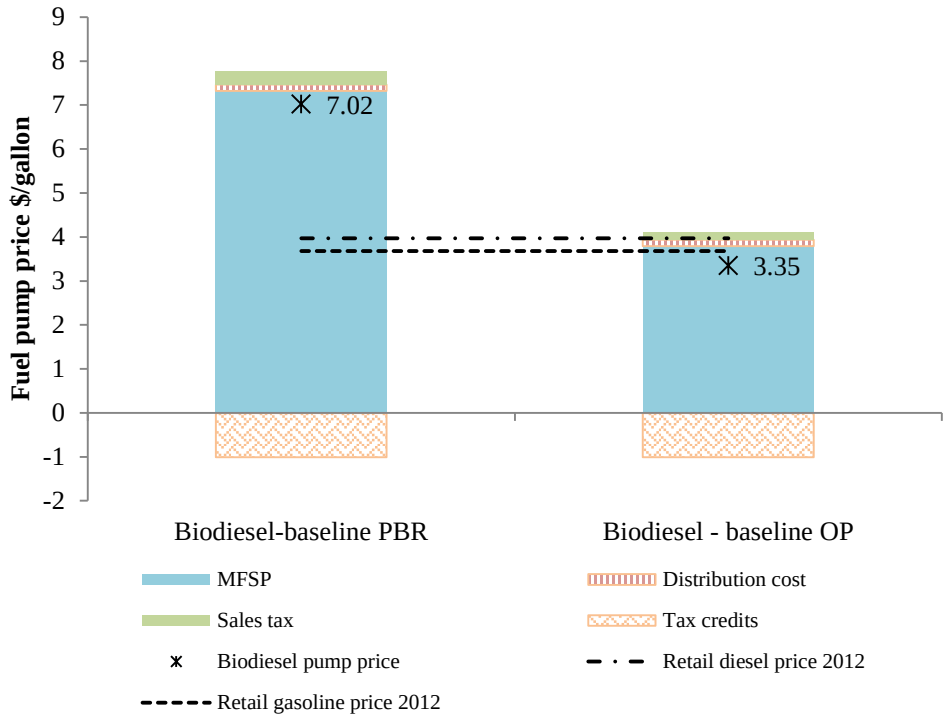

Fig. 7. Comparison of pump price of the biodiesel from PBR and OP scenarios, with the conventional diesel retail price (dashed line) and gasoline retail price (dotted line).

4.3. Environmental impacts

Figs. 8a and b illustrate the overall net GHG emissions of diesel and gasoline and their contribution analysis. The 'above-the-line' scores are environmental burdens, whilst the 'below-the-line' ones are biogenic carbon sequestered in biomass feedstock and GHG credits from surplus steam in Pyrolysis (Section 100), Upgrading (Section 200) and Hydrocracking (Section 500). As shown in Figs. 8a and 8b, the biggest score from the *vehicle operation* is the emissions from fuel combustion and the second biggest is the flue gas exhaust from CCS, (Section 400). They are partially offset by biomass carbon sequestration, because carbon in the biofuel is biogenetic carbon that was originally sequestered in biomass feedstock. The emissions from algae cultivation and anaerobic digestion are mainly from the production of nutrients and electricity. For PBR scenario, the emissions from biomass production and harvesting are small and only account for 12.9% for diesel and 16.5% for gasoline, respectively. Similar measures for the OP scenario are 9.7% and 9.6% respectively for diesel and gasoline. Overall, the net 'well-to-wheel' GHG emissions are 0.05 kg CO_2 eq./km for diesel and 0.02 CO_2 eq./km for

gasoline for the PBR scenario whilst the net GHG emissions for the OP scenario are 0.07 kg CO_2 eq./km for diesel and 0.04 kg CO_2 eq./km for gasoline. These results are compared with 'well-to-wheel' GHG emissions for diesel and gasoline reported by Hsu, [93] for stand-alone biomass pyrolysis process and that for refinery gasoline in Fig. 9a. The implication is that for the OP scenario, the GHG emissions for diesel and gasoline are reduced by 50% and 70% respectively compared to equivalent measures corresponding to the biomass pyrolysis stand-alone. In addition, the GHG emissions factor for gasoline in the present study is around 15% of that for refinery gasoline. The PBR scenario delivers higher GHG emissions reductions (65% for diesel and 84% for gasoline) compared to the biomass pyrolysis stand-alone and results in a GHG emission factor for gasoline which is 7% of that for refinery gasoline. Similarly, Fig. 9b shows the 'Well-to-Gate' (from biomass cultivation to fuels production) GHG emissions for diesel and gasoline in the present study compared to those in Hsu's study [93] for biomass-derived diesel and Frank, *et al.*'s study [76] for algae-derived diesel using OP system. It is found that GHG emissions factors for diesel in our PBR scenario are 65% and 64% smaller than those in Hsu, [93] and Frank, *et al.*'s [76] studies, respectively. In the OP scenario, these numbers are 51% and 49% respectively. The overall observation is that the integrated process can deliver significantly better GHG results than the stand-alone poplar pyrolysis plant and the stand-alone algae diesel plant. Moreover, the GHG emissions reduction of the biodiesel produced from the proposed integrated biorefinery can fulfil the threshold of 50% for biomass-based biodiesel regulated by Renewable Fuel Standards [92].

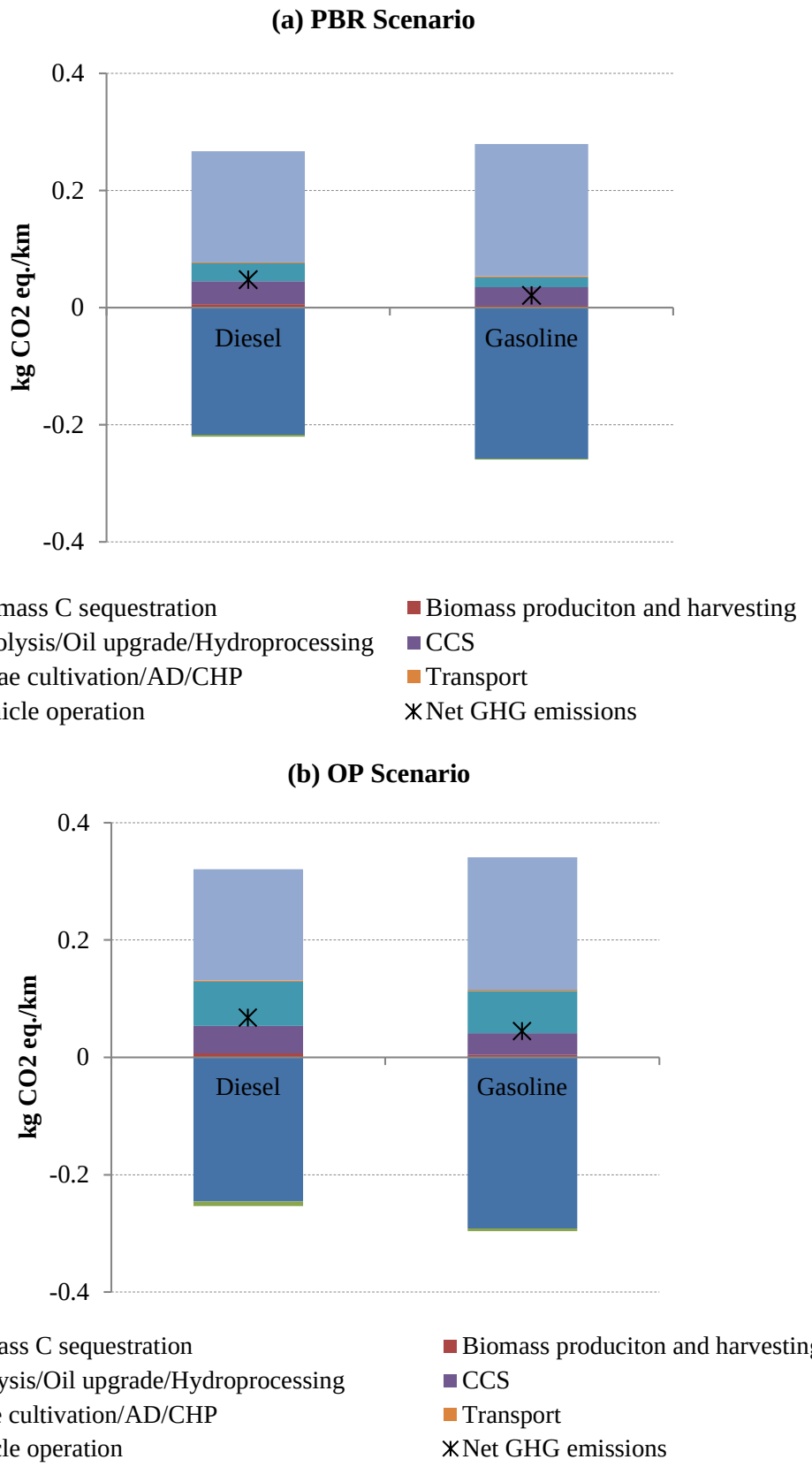

Figs. 8. GHG emissions of diesel and gasoline (Unit '1km travelled by a light-duty passenger vehicle')

This article should be cited as: Sharifzadeh M*, Wang L, Shah N, (2015). Integrated bio-refineries: CO_2 utilization for maximum biomass conversion. *Renewable and Sustainable Energy Reviews*, 47, 151–161, (Link).

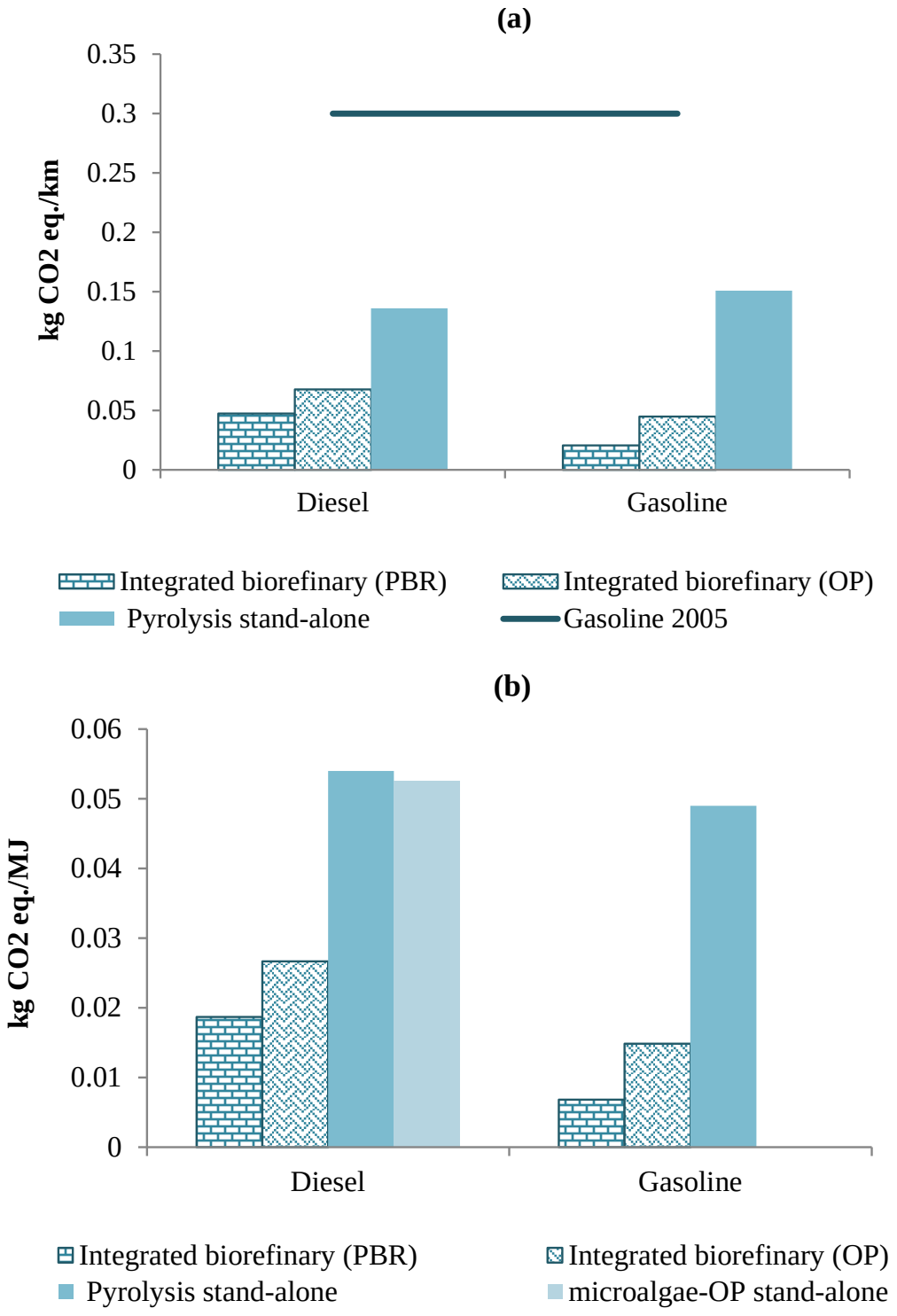

Figs. 9. Comparison with other studies: (a) 'Well-to-Wheel' Unit '1km travelled by a light-duty passenger vehicle'); (b) 'Well-to-Gate' Unit: '1MJ of fuel')

5. Discussions and conclusion

The inherent chemistry of biomass poses an important challenge toward producing liquid fuels *i.e.*, a large amount of biomass carbon should be removed as carbon dioxide in order to adjust the effective hydrogen to carbon ratio to a level compatible with the current energy infrastructure. Therefore, CO_2 utilization is essential for sustainability of future biorefineries. The present study explored the techno-economic and life-cycle assessment of an important instance of future integrated biorefineries, in which the carbon dioxide produced during biomass pyrolysis and upgrading is utilized for microalgae cultivation. Such process integration is motivated by the inherent synergies through bio-oil upgrading and refining, and minimization of the costs associated with CO_2 capture and hydrogen production. The proposed biorefinery has profound environmental impacts, because firstly, based on the same amount of biomass, it produces significantly higher amount of fuel. The implication is less deforestation and environmental protection. Secondly, the amount of emitted CO_2 is substantially reduced from 45% of initial carbon to only 6%. The implication is that the contribution of the produced fuel to decarbonisation of the transportation infrastructure is almost an order of magnitude higher than the equivalent standalone pyrolysis process. Finally, the extra produced fuel can compensate the cost of CO_2 utilization, and is still competitive with respect to petroleum-derived fuel. Furthermore, there are plenty of opportunities to improve the economic and environmental performance of the proposed integrated scheme. With respect to carbon conversion, it was shown that the GHG emissions can be suppressed to as low as 6%. However, still a large amount (19%) of carbon is converted to fertilizer (biomass residues). This is because the lipid content of microalgae is as low as 25% and only less than half of the microalgae is anaerobically digestible. Therefore, improving the lipid yield and the anaerobic digestion efficiency has the potential to enhance the overall biomass conversion. Furthermore, there is an important trade-off between the costs of bioreactor and carbon emission, and commercializing more efficient and economic bioreactors is highly desirable. The integrated biorefinery may also benefit from new upgrading methods that can co-process the bio-oil and extracted lipids. All these in addition to cheaper methods for carbon capture will benefit commercialization of the proposed integrated biorefineries.

This article should be cited as: Sharifzadeh M*, Wang L, Shah N, (2015). Integrated bio-refineries: CO_2 utilization for maximum biomass conversion. *Renewable and Sustainable Energy Reviews*, 47, 151–161, (Link).

6. Acknowledgements

Mahdi Sharifzadeh thanks the financial supports of Carbon Trust (CT) and Department of Energy & Climate Change (DECC) for his postdoctoral studies.

7. Nomenclature

AD	anaerobic Digestion
ANL	Argonne National Laboratory
CCS	Carbon capture and storage
DOE	Department of Energy
F_{scale}	The exponent used for scaling equipment costs
GHG	greenhouse gas
LCA	Life cycle analysis
MACRS	Modified Accelerated Cost Recovery System
MEA	Monoethanolamine
MFSP	minimum fuel selling price
NREL	National Renewable Energy Laboratory
OP	open ponds
PBR	photobioreactor
TCI	Total Capital Investment
TIC	Total Installed Cost
tpd	ton per day
TPEC	Total Purchased Equipment Cost

8. References

[1] Panwara NL, Kaushik SC, Kothari S. Role of renewable energy sources in environmental protection: A review. Renew Sust Energ Rev, 2011; 15: 1513–1524.

[2] Turconi R, Boldrin A, Astrup T. Life cycle assessment(LCA)of electricity generation technologies: Overview, comparability and limitations. Renew Sust Energ Rev, 2013; 28: 555–565.

[3] Luque R, Lovett J C, Datta B, Clancy J, Campelo J M, Romero A A. Biodiesel as feasible petrol fuel replacement: a multidisciplinary overview. Energy Environ Sci, 2010; 3: 1706-1721.

[4] Serrano-Ruiz J C, Dumesic J A. Catalytic routes for the conversion of biomass into liquid hydrocarbon transportation fuels. Energy Environ Sci, 2011; 4: 83-99.

[5] Williams PJleB, Laurens LML. Microalgae as biodiesel & biomass feedstocks: Review &

analysis of the biochemistry, energetics & economics. Energy Environ Sci, 2010; 3: 554-590.

[6] Ahmad AL, Mat Yasin NH, Derek CJC, Lim JK. Microalgae as a sustainable energy source for biodiesel production: A review. Renew Sust Energ Rev, 2011; 15: 584–593.

[7] Wang L, Sharifzadeh M, Templer R, R J Murphy. Technology performance and economic feasibility of bioethanol production from various waste papers. Energy Environ Sci, 2012; 5: 5717-5730.

[8] Wang L, Sharifzadeh M, Templer R, Murphy R J. Bioethanol production from various waste papers: Economic feasibility and sensitivity analysis. Appl Energ, 2013; 111: 1172–1182.

[9] Martinez JD, Puy N, Murillo R, Garcıa T, Navarro MV, Mastral AM. Waste tyre pyrolysis–A review. Renew Sust Energ Rev, 2013; 23: 179–213.

[10] Fonts I, Gea G, Azuara M, Ábrego J, Arauzo J. Sewage sludge pyrolysis for liquid production: A review. Renew Sust Energ Rev, 2012; 16: 2781– 2805.

[11] Naik SN, Goud VV, Rout PK, Dalai AK. Production of first and second generation biofuels: A comprehensive review. Renew Sust Energ Rev, 2010; 14: 578–597.

[12] Anex R P, Aden A, Kabir Kazi F, Fortman J, Swanson R M, Wright M M, Satrio J A, Brown R C, Daugaard D E, Platon A, Kothandaraman G, Hsu D D, Dutta. A Techno-economic comparison of biomass-to-transportation fuels via pyrolysis, gasification, and biochemical pathways. Fuel, 2010; 89: S29–S35.

[13] Bridgwater A V, Toft A J, Brammer J G. A techno-economic comparison of power production by biomass fast pyrolysis with gasification and combustion. Renew Sust Energ Rev, 2002; 6: 181–248.

[14] Vispute T P, Zhang H, Sanna A, Xiao R, Huber G W. Renewable Chemical Commodity Feedstocks from Integrated Catalytic Processing of Pyrolysis Oils. Science, 2010; 330: 1222.

[15] Mettler M S, Vlachos D G, Dauenhauer P J. Top ten fundamental challenges of biomass pyrolysis for biofuels. Energy Environ Sci, 2012; 5: 7797.

[16] Azeez A M, Meier D, Odermatt J, and Willner T. Fast Pyrolysis of African and European Lignocellulosic Biomasses Using Py-GC/MS and Fluidized Bed Reactor. Energy Fuels, 2010; 24: 2078–2085.

[17] Ben H, Ragauskas A J. NMR Characterization of Pyrolysis Oils from Kraft Lignin. Energy Fuels, 2011; 25: 2322–2332.

[18] Ben H, Ragauskas AJ. Comparison for the compositions of fast and slow pyrolysis oils by NMR Characterization. Bioresour Technol, 2013; 147: 577–584.

[19] White J E, Catallo W J, Legendre B L. Biomass pyrolysis kinetics: A comparative critical review with relevant agricultural residue case studies. J Anal Appl Pyrol, 2011; 91: 1–33.

[20] Papadikis K, Gu S, Bridgwater AV, Gerhauser H. Application of CFD to model fast pyrolysis of biomass. Fuel Process Technol, 2009; 90: 504–512.

[21] Isahak WNRW, Hisham MWM, Yarmo MA, Hin TY. A review on bio-oil production from biomass by using pyrolysis method. Renew Sust Energ Rev, 2012; 16: 5910–5923.

[22] Motasemi F, Afzal MT. A review on the microwave-assisted pyrolysis technique. Renew Sust Energ Rev, 2013; 28: 317–330.

[23] Borges FC, Du Z, Xie Q, Trierweiler JO, Cheng Y, Wan Y, Liu Y, Zhu R, Lin X, Chen P, Ruan R. Fast microwave assisted pyrolysis of biomass using microwave Absorbent. Bioresour Technol, 2014; 156: 267–274.

[24] Akhtar J, Amin NS. A review on operating parameters for optimum liquid oil yield in biomass pyrolysis. Renew Sust Energ Rev, 2012; 16: 5101–5109.

[25] Zhang L, Liu R, Yin R, Mei Y. Upgrading of bio-oil from biomass fast pyrolysis in China: A review. Renew Sust Energ Rev, 2013; 24: 66–72.

[26] Sadhukhan J. Multiscale simulation for high efficiency biodiesel process intensification. Computer Aided Chemical Engineering, 2012; 30: 1023-1027.

[27] Brown T R, Thilakaratne R, Brown R C, Hu G. Techno-economic analysis of biomass to transportation fuels and electricity via fast pyrolysis and hydroprocessing. Fuel, 2013; 106: 463–469.

[28] Wright M M, Daugaard D E, Satrio J A, Brown R C. Techno-economic analysis of biomass fast pyrolysis to transportation fuels. Fuel, 2010; 89: S2–S10.

[29] Gebreslassie B H, Slivinsky M, Wang B, You F. Life cycle optimization for sustainable design and operations of hydrocarbon biorefinery via fast pyrolysis, hydrotreating and hydrocracking. Comput Chem Eng, 2013; 50: 71– 91.

[30] Kim J, Realff M J, Lee J H, Whittaker C, Furtner L. Design of biomass processing network for biofuel production using an MILP model. Biomass Bioenergy, 2011; 35: 853-871

[31] Akgul O, Shah N, Papageorgiou L G. Economic optimisation of a UK advanced biofuel supply chain. Biomass Bioenergy, 2012; 41: 57–72.

[32] Braimakisa K, Atsoniosa K, Panopoulos KD, Karellas S, Kakaras E, Economic evaluation of decentralized pyrolysis for the production of bio-oil as an energy carrier for improved logistics towards a large centralized gasification plant. Renew Sust Energ Rev, 2014; 35: 57–72.

[33] Meier D, B Beld, Bridgwater AV, Elliott DC, Oasmaa A, Preto F State-of-the-art of fast pyrolysis in IEA bioenergy member countries. Renew Sust Energ Rev, 2013; 20: 619–641.

[35] Jenkins B M, Baxter L L, Miles Jr T R, Miles T R. Combustion properties of biomass. Fuel Processing Technology, 1998; 54: 17–46.

[36] Floudas C A, Elia J A, Baliban R C. Hybrid and single feedstock energy processes for liquid transportation fuels: A critical review. Comput Chem Eng, 2012; 41: 24– 51.

[37] Kreutz T G, Larson E D, Liuand G, Williams R H. Fischer–Tropsch Fuels from Coal and Biomass. Proc of the 25th intl Pittsburg coal conf 2008.

[38] Chmielniak T, Sciazko M. Co-gasification of biomass and coal for methanol synthesis. Appl Energ, 2003; 74: 393–403.

[39] Li H, Hong H, Jin H, R Cai. Analysis of a feasible polygeneration system for power and methanol production taking natural gas and biomass as materials. Appl Energ, 2010; 87: 2846–2853.

[40] Marker T, Petri J, Kalnes T, McCall M, Mackowiak D, Jerosky B, Reagan B, Nemeth L,

Krawczyk M, Czernik S, Elliott D, D Shonnard. Opportunities for biorenewables in oil refineries UOP, Technical Report.

[41] de Miguel Mercader F, Groeneveld M J, Kersten S R A, Way N W J, Schaverien C J, Hogendoorn J A. Production of advanced biofuels: Co-processing of upgraded pyrolysis oil in standard refinery units. Appl Catal B, 2010; 96: 57–66.

[42] Ng K S, Zhang N, Sadhukhan J. Techno-economic analysis of polygeneration systems with carbon capture and storage and CO reuse. Chem Eng J, 2013; 219: 96–108.

[43] Ragauskas J, Williams C K, Davison B H, Britovsek G, Cairney J, Eckert C A, Frederick Jr W J, Hallett J P, Leak D J, Liotta C L, Mielenz J R, Murphy R, Templer R, Tschaplinski T. The Path Forward for Biofuels and Biomaterials. Science, 2006; 311: 484-489.

[44] de Vyver S V, Roman-Leshkov Y. Emerging catalytic processes for the production of adipic acid. Catal Sci Technol, 2013; 3: 1465—1479.

[45] Bozell J J, Petersen G R. Technology development for the production of biobased products from biorefinery carbohydrates—the US Department of Energy's "Top 10" revisited. Green Chem, 2010; 12: 539–554.

[46] Boot-Handford M E, Abanades J C, Anthony E J, Blunt M J, Brandani S, Mac Dowell N, Fern´andez J R, Ferrari M-C, Gross R, Hallett J P, Haszeldine R S, Heptonstall P, Lyngfelt A, Makuch Z, Mangano E, Porter R T J, Pourkashanian M, Rochelle G T, Shah N, Yao J G, Fennell P S. Carbon capture and storage update. Energy Environ Sci, 2014; 7: 130.

[47] Bhown A S, Freeman B C. Analysis and Status of Post-Combustion Carbon Dioxide Capture Technologies. Environ Sci Technol 2011; 45: 8624–8632.

[48] Hadjipaschalis I, Kourtis G, Poullikkas A. Assessment of oxyfuel power generation technologies. Renew Sust Energ Rev, 2009; 13: 2637–2644.

[49] Scholz M, Melin T, Wessling M. Transforming biogas into biomethane using membrane technology. Renew Sust Energ Rev, 2013; 17: 199–212.

[50] Abd Rahaman MS, Cheng L, Xu X, Zhang L, Chen H. A review of carbon dioxide capture and utilization by membrane integrated microalgal cultivation processes. Renew Sust

Energ Rev, 2011; 15: 4002–4012.

[51] Lee ZH, Lee KT, Bhatia S, Mohamed AR. Post-combustion carbon dioxide capture: Evolution towards utilization of nanomaterials. Renew Sust Energ Rev, 2012; 16: 2599–2609.

[52] Wang M, Lawal A, Stephenson P, Sidders J, Ramshaw C. Post-combustion CO capture with chemical absorption: A state-of-the-art review. Chem Eng Res Des, 2011; 89: 1609–1624.

[53] Markewitz P, Kuckshinrichs W, Leitner W, Linssen J, Zapp P, Bongartz R, Schreiber A, Müller T E. Worldwide innovations in the development of carbon capture technologies and the utilization of CO2. Energy Environ Sci, 2012; 5: 7281-7305

[54] Aresta M, Dibenedetto A, Angelini. A The changing paradigm in CO2 utilization. Journal of CO2 Utilization, 2013; 3–4: 65–73.

[55] Sharma Y C, Singh B, Korstad J A. critical review on recent methods used for economically viable and eco-friendly development of microalgae as a potential feedstock for synthesis of biodiesel. Green Chem, 2011; 13: 2993.

[56] Pires JCM, Alvim-Ferraz MCM, Martins FG, Simões M. Carbon dioxide capture from flue gases using microalgae: Engineering aspects and biorefinery concept. Renew Sust Energ Rev, 2012; 16: 3043– 3053.

[57] Liu J, Mukherjee J, Hawkes J J, Wilkinson S J. Optimization of lipid production for algal biodiesel in nitrogen stressed cells of Dunaliella salina using FTIR analysis. J Chem Technol Biotechnol and Biotechnology, 2013; 88: 1807–1814.

[58] Huang G, Chen G, Chen F. Rapid screening method for lipid production in alga based on Nile red fluorescence. Biomass Bioenergy, 2009; 33: 1386–1392.

[59] Show K, Lee D, Chang J. Algal biomass dehydration. Bioresour Technol, 2013; 135: 720–729.

[60] Elliott D C, Hart T R, Schmidt A J, Neuenschwander G G, Rotness L J, Olarte M V, Zacher A H, Albrecht K O, Hallen R T, Holladay J E. Process development for hydrothermal liquefaction of algae feedstocks in a continuous-flow reactor. Algal Research, 2013; 2:

445–454.

[61] Wang K, Brown R C. Catalytic pyrolysis of microalgae for production of aromatics and ammonia. Green Chem, 2013; 15: 675–681.

[62] Bai X, Ghasemi Naghdi F, Ye L, Lant P, Pratt S. Enhanced lipid extraction from algae using free nitrous acid pretreatment. Bioresour Technol, 2014; 159: 36–40.

[63] Thangalazhy-Gopakumar, S, Adhikari, S, Chattanathan SA, Gupta RB. Catalytic pyrolysis of green algae for hydrocarbon production using H+ZSM-5 Catalyst. Bioresour Technol, 2012; 118: 150-157.

[64] Vardon, DR, Sharma, BK, Blazina, GV, Rajagopalan, K, Strathmann, TJ. Thermochemical conversion of raw and defatted algal biomass via hydrothermal liquefaction and slow pyrolysis. Bioresour Technol, 2012; 109: 178–187.

[65] Wu K, Liu, J, Wu, Y, Chen, Y, Li, Q. Xiao, X, Yang, M,. Pyrolysis characteristics and kinetics of aquatic biomass using thermogravimetric analyser. Bioresour Technol, 2014; 163: 18–25.

[67] Ruiz HA, Rodriguez-Jasso RM, Fernandes, BD, Vicente AA, Teixeira JA. Hydrothermal processing, as an alternative for upgrading agriculture residues and marine biomass according to the biorefinery concept: A review. Renew Sust Energ Rev, 2013; 21: 35–51.

[68] Sialve B, Bernet N, Bernard O. Anaerobic digestion of microalgae as a necessary step to make microalgal biodiesel sustainable. Biotechnol Adv, 2009; 27: 409–416.

[69] Wang, T, Yabar, H, Higano, Y,. Perspective assessment of algae-based biofuel production using recycled nutrient sources: The case of Japan. Bioresour Technol, 2013; 128: 688–696.

[70] Bulgariu D, Bulgariu L. Equilibrium and kinetics studies of heavy metal ions biosorption on green algae waste biomass. Bioresour Technol, 2012; 103: 489–493.

[71] Brennan L, Owende P. Biofuels from microalgae—A review of technologies for production, processing, and extractions of biofuels and co-products. Renew Sust Energ Rev, 2010; 14:

557–577.

[72] Mata TM, Martins AA, Caetano NS. Microalgae for biodiesel production and other applications: A review. Renew Sust Energ Rev, 2010; 14: 217–232.

[73] Singh J, Gu S. Commercialization potential of microalgae for biofuels production. Renew Sust Energ Rev, 2010; 14: 2596–2610.

[74] Jones S B, Holladay JE, Valkenburg C, Stevens D J, Walton C W, Kinchin C, Elliott D C, Czernik S. Production of Gasoline and Diesel from Biomass via Fast Pyrolysis, Hydrotreating and Hydrocracking: A Design Case. US Department of Energy 2009; Technical Report.

[75] Davis R, Aden A, Pienkos PT Techno-economic analysis of autotrophic microalgae for fuel production. Appl Energ, 2011; 88: 3524–3531.

[76] Frank E D, Han J, Palou-Rivera I, Elgowainy A, Wang M Q. Life-cycle analysis of algal lipid fuels with the greet model, Argonne National Laboratory, 2011, Technical Report.

[77] gCCS: Whole chain CCS systems modelling, Process Systems Enterprise (Accessed Jan 2015, http://www.psenterprise.com/power/ccs/gccs.html).

[78] Sharifzadeh, M, Shah, N, (2014). Seamless integration of solvent-based carbon capture processes into natural gas combined cycle (NGCC) plants: rigorous modelling, optimization and operability analysis, Oral presentation at AIChE Annual Meeting 2014, (Link).

.

[79] Abanades J C, Rubin E S, Anthony E J. Sorbent cost and performance in CO2 capture systems. Ind Eng Chem Res, 2004; 43: 3462-3466.

[80] COSTWater, running costs of wastewater treatment plant, URL: http://www.costwater.com/runningcostwastewater.htm, Accessed May, 2014.

[81] US Energy Information Administration, Natural Gas Prices, 2013a, URL: http://www.eia.gov/dnav/ng/ng_pri_sum_dcu_nus_a.htm, Accessed May, 2014.

[82] US Energy Information Administration, Electricity Wholesale Market, Data, 2013b, URL:

http://www.eia.gov/electricity/wholesale/, Accessed May, 2014.

[83] Aspen Plus software tool, V8.4. Apsen Tech.

[84] Phillips S, Aden A, Jechura J, Dayton D, Eggeman T. Thermochemical Ethanol via Indirect Gasification and Mixed Alcohol Synthesis of Lignocellulosic Biomass 2007, National Renewable Energy Laboratory (NREL), Thermochemical Ethanol via Indirect Gasification and Mixed Alcohol Synthesis of Lignocellulosic Biomass, Technical Report, NREL/TP-510-41168.

[85] Slade R. Prospects for cellulosic ethanol supply-chains in Europe: a technoeconomic and environmental assessment, PhD Thesis 2009, Imperial College of Science, Technology and Medicine

[86] Wikipedia, Sales taxes in the United States, http://en.wikipedia.org/wiki/Sales_taxes_in_the_United_States, Accessed May, 2014.

[87] Wikipedia, Fuel tax, http://en.wikipedia.org/wiki/Fuel_tax#United_States, Accessed May, 2014.

[88] Yacobucci BD. Biofuels Incentives: A Summary of Federal Programs 2012 Congressional Research Service.

[89] EIA, Weekly retail gasoline and diesel prices http://www.eia.gov/dnav/pet/pet_pri_gnd_dcus_nus_a.htm , Accessed May, 2014.

[90] Gasol C M, Gabarrell X, Anton A, Rigola M, Carrasco J, Ciria P, Rieradevall J. LCA of poplar bioenergy system compared with Brassica carinata energy crop and natural gas in regional scenario. Biomass Bioenergy, 2009; 33: 119–129.

[91] Jungbluth N, Faist Emmenegger M, Dinkel F, Stettler C, Doka G, Chudacoff M, Dauriat A, Gnansounou E, Sutter J, Spielmann M, Kljun N, Keller M, K Schleiss. Life cycle inventories of Bioenergy 2007, Swiss Centre for Life Cycle Inventories, Dübendorf.

[92] IPCC, IPCC Guidelines for National Greenhouse Gas Inventories Hayama, Kanagawa, Japan: Institute for Global Environmental Strategies, 2006.

[93] Hsu D D. Life Cycle Assessment of Gasoline and Diesel Produced via Fast Pyrolysis and Hydroprocessing, 2011, NREL Technical Report NREL/TP-6A20-49341.

Integrated biorefineries: CO_2 utilization for maximum biomass conversion

Mahdi Sharifzadeh[a1] , Lei Wang[b] and Nilay Shah[a]

[a] Centre for Process Systems Engineering (CPSE), Department of Chemical Engineering, Imperial College London. [b] Centre for Environmental Policy, Imperial College London.

Electronic Supplementary Material

The present document is prepared to complement Sections 2.4 and 3.2 in the manuscript. The features of interest include the process descriptions and the flow diagrams of the sub-processes (Sections 100-800 in Figs. 21 and 2b), and a list of detailed equipment cost in Table S1 and S2. More detail can be found in the corresponding references.

Section 100: Biomass pyrolysis

The process flow diagram for the pyrolysis section is shown in Fig. S1, adapted from Jones *et al*., [S1]. The feedstock of this section is hybrid poplar and the product is the pyrolysis oil, also called biooil, which is sent to Section 200 for upgrading. The exhaust gases from this section are sent to Section 400 for carbon capture. The produced ash is landfilled. All the modelling assumptions in this section are based on Jones *et al*.'s study [S1].

Section 200: Crude oils upgrading

The mission of Section 200 is upgrading the biooil from biomass pyrolysis in addition to the microalgae lipids from Section 700. The process flow diagram for this section is shown in Fig. S2. The upgrading yields and the product composition of the two-stage biooil upgrading were adapted from Jones *et al*., [S1]. Similarly, the yield and product composition of the lipids upgrading reactor

[1] Corresponding Author: Dr Mahdi Sharifzadeh; Room C603, Roderic Hill Building, South Kensington Campus, Imperial College London, UK. SW7 2AZ. E-mail: mahdi@imperial.ac.uk; Tel: +44(0)7517853422

were adapted from Table 3 of Davis *et al.*'s study, [S2]. According to this publication, the lipid upgrading reactions were conducted at 350^{o}C and 500 psig. The hydrogen feed is 1.5% (mass basis) of the reactor feed. 80% of the feed is converted to fuel (78% Diesel, and 2% naphtha). The remaining products are 2% H2O, 11% CO2, 1% CO and 6% propane. The yield and hydrogen requirements of the pyrolysis oil hydrotreatment reactors (R-202 and R-203) were adopted from Table A.2 of Jones, *et al.*'s study [S1]. The upgraded products are firstly separated from the associated light gases and water and then are sent to Section 300 for further refining and upgrading. The light gases are sent for hydrogen production to Section 600. The oily-water is sent for wastewater treatment.

Sections 300 & 500: Separation and hydrocracking

The flow diagram for Sections 300 and 500 is shown in Fig. S3. The upgraded effluent are further refined in Section 300 through a sequence of distillation columns. Any dissolved light gases are separated and sent to Section 600 for hydrogen production. The heavy fraction is sent to the hydrocracking Section 500 and the lighter fractions are separated as gasoline and diesel. The hydrocracking yield and hydrogen requirement were adopted from Table A.3 of Jones, *et al.*'s study [S1]. In addition, the specifications of the distillations columns were adjusted so the gasoline and diesel products have the same quality as this study [S1].

Section 400: Carbon Capture and Storage (CCS)

This section is shown in Fig. S4. The CO_2 is firstly separated in a sequence of absorption and desorption columns using monoethanolamine (MEA) solvent. The separated CO_2 is compressed in a compressor train and stored in a liquefied state under pressure, during the night. Then during the day, the stored CO_2 is expanded in a sequence of turbo-expanders in order to produce power and simultaneously expand to the operating condition needed for microalgae cultivation. The capture process model (left dotted square in Figure S4) was developed using gCCS software tool [S3]. The column model was based on two-film theory and statistical associating fluid theory for potentials of variable range (SAFT-VR). Four parallel carbon capture trains were considered. The specifications of the CO_2 compression and storage processes were adapted from a study conducted by DOE/NETL [S4].

Section 600: Hydrogen production

The required hydrogen for hydrogenation of biooil and lipids, as well as hydrocracking of heavy residues is produced by reforming natural gas and by-product light gases. The flow diagram of Section 600 is shown in Fig. S5. The modelling assumptions of this section are based on Jones' *et al*.,'s study [S1]. The reformer reactor was modelled based on chemical equilibrium (Gibbs free energy minimization). The efficiency of the pressure swing adsorption unit was 90%.

Sections 700 & 800: Microalgae cultivation and anaerobic digestion (AD)

The captured CO_2 was fed to Section 700 (Fig. S6) for microalgae cultivation. Two scenarios of (i) Photobioreactors (PBRs) and (ii) Open Ponds (OPs) are studied and compared. The algea cutivation medium is sent to a sequence of mechanical separation steps for dewatering including settling, flocculation, and centrifugation. Then, using high pressure homogenization and solvent extraction, its lipid content is separated and sent for to Section 200 for upgrading. The lipid extracted algae is sent to Section 800 for Anaerobic Digestion and biogas production.

The main constituents of algae biomass are lipids, protein, and carbohydrates and depending on the algae strain and cultivation strategy, their composition varies significantly as 17.5-38.5% for lipids, 6.7-28.2 % for protein, 49.5-52.9% for carbohydrates, on mass basis, correspondingly [S6]. In the present research, the conservative values of 25% lipids, 25% proteins, and 50% carbohydrates were considered for the algae composition. This is also consistent with Davis *et al*.'s study, [S2] (table 2 of that publication).The modelling assumptions of the photobioreactor were adapted from Davis *et al*., [S2], as outlined in Section 2 and summarized at Tables 2 and 3 of that publication. According to this publication, the solid loading of the algae cultivation medium leaving the settling tank is as low as 10 g/L, and then it is dewatered using flocculants such as chitosan to 100 g/L. Later, the centrifugation step increases the slurry's concentration to 200 g/L. Finally, the lipid extraction is achieved by a combination of mechanical high pressure homogenization and solvent extraction. The energetic requirement of each mechanical step was adapted from Table 15 of Frank, *et al*., [S5]. The required data for modelling the Anaerobic Digestion (AD) process in Section 800 (Fig. S7) were adapted from Table 7 by Frank *et al*., [S5]. According to this publication, each gram of total solid (lipid extracted

algae) can be digested to produce 0.3 litre of methane. The concentration of methane in the biogas is 67% on the volumetric basis, which is equivalent to 43.3% on the mass basis. The rest is carbon dioxide and the mixture is saturated with water.

Economic analysis approach

The detailed costs of process equipment are reported in Tables S1 and S2. As explained in the manuscript, the method of costing for conventional process equipment (distillations, pumps, etc.) was based on the simulation data and was calculated using Aspen Economic Analyzer. However, for nonconventional equipment, such as reformer, reactors, etc. the costing was based on scaling with respect to data from literature [S1, S2, S4]: $\textbf{New cost} = \textbf{Base cost} * \left(\frac{\textbf{New size}}{\textbf{Base size}}\right)^{f_{scale}}$

In particular, in CCS section 400, the costs of the whole capture process (left dotted square in Figure S4 including water wash, absorber, and desorber columns) was calculated with respect to data from reference [S4].

References

[S1] Jones S B, Holladay JE, Valkenburg C, Stevens D J, Walton C W, Kinchin C, Elliott D C, Czernik S. Production of Gasoline and Diesel from Biomass via Fast Pyrolysis, Hydrotreating and Hydrocracking: A Design Case. US Department of Energy 2009; Technical Report.

[S2] Davis R, Aden A, Pienkos PT Techno-economic analysis of autotrophic microalgae for fuel production. Appl Energ, 2011; 88: 3524–3531.

[S3] gCCS: Whole chain CCS systems modelling, Process Systems Enterprise (Accessed Jan 2015, http://www.psenterprise.com/power/ccs/gccs.html).

[S4] DOE, Cost and Performance Baseline for Fossil Energy Plants Volume 1: Bituminous Coal and Natural Gas to Electricity, 2010, Technical Report, DOE/NETL-2010/1397.

[S5] Frank E D, Han J, Palou-Rivera I, Elgowainy A, Wang M Q. Life-cycle analysis of algal lipid fuels with the greet model, Argonne National Laboratory, 2011, Technical Report.

[S6] Lardon L, Hélias A, Sialve B, Steyer J, Bernard O, Life-Cycle Assessment of biodiesel production from microalgae. Environ. Sci. Technol., 2009, 43 (17), 6475–6481.

1 **Table S1 Key equipment capital cost in PBR scenario**

Equipment Label	Equipment Name	Original Stream Metric	New Stream Metric	Scaling Units	Size Ratio	Scaling Exp	Installed Factor	Installed Equip Cost at original Metric in base year	Installed Equip Cost at new metric in 2012$
Section 100 Pyrolysis									
	Feedstock handling	2,000	2,000	tpd	1	0.7	2.47	$19,212,106	$21,687,667
R101	Pyrolyzer	2,000	2,000	tpd	1	0.7	2.47	$11,699,724	$13,207,283
V102	Quench	2,000	2,000	tpd	1	0.7	2.47	$6,691,470	$7,553,694
	Product recovery and storage incl. cyclone, vessel, pump and cooler	2,000	2,000	tpd	1	0.7	2.47	$2,759,369	$3,114,925
	Recycle incl. sand recycle, compressor, demister	2,000	2,000	tpd	1	0.7	2.47	$4,759,911	$5,373,246
								Total	$50,936,815
Section 200 Upgrading									
R201	Lipid hydrotreater *	1,959	816	scfh	0.42	0.65	2.47	$2,120,904	$1,354,987
R202	First stage pyrolysis oil hydrotreater	1,959	1,959	scfh	1	0.65	2.47	$2,120,904	$2,394,191
R203	Second stage pyrolysis oil hydrotreater	1,959	1,959	scfh	1	0.65	2.47	$22,221,810	$25,085,184
PSA-201	PSA	15	15	mmscfd H2	1	0.65	2.47	$ 2,694,155	$3,041,308
E202	Heat exchanger	38	38	mmbtuh	1	0.65	2.47	$1,347,791	$1,521,395
F202	Fired heater	40	40	mmbtuh	1	0.65	2.47	$3,057,432	$3,451,395
C201	Hydrogen compressor	2,840	2,840	acfm	1	0.65	2.47	$10,746,045	$12,130,718
	Others								$6,234,279
								Total	$55,213,457
Section 300 Separation & Section 500 Hydro cracking									
T301	Debutanizer	69,495	96,792	lb/h	1.39	0.65	2.47	$222,238	$311,159
T302	Naphtha Splitter	66,028	90,822	lb/h	1.38	0.65	2.47	$488,894	$678,975
T303	Diesel Splitter	46,668	73,984	lb/h	1.59	0.65	2.47	$184,801	$281,462
T304	Product Splitter	9,694	15,178	lb/h	1.57	0.65	2.47	$344,139	$519,917
R501	Hydrocracker Unit	7,473	10,685	cuf/h	1.43	0.65	2.47	$14,130,726	$20,125,142
	Others								$2,155,028
								Total	$24,071,683
Section 400 Carbon capture, storage and expansion									
	Absorption and desorption unit a	1,316,349	254,050	lb/h	0.19	0.6	2.47	$218,463,000	$91,906,165
C401a-f	CO_2 compressors *								$10,900,000
Exp401a-c	CO_2 expanders *								$1,665,300
	Others								$4,977,800
								Total	$109,449,265

2

Table S1. Continued

Section 600 Hydrogen plant									
	Steam reformer system	3460	3896	kg/h	1.13	0.65	2.47	$87,152,793	$106,272,774
								Total	$106,272,774
Section 700 Microalgae cultivation and anaerobic digestion									
	Photobioreactor system b	10	37	MM gallon/ year	3.7	0.65	2.47	$522,000,000	$1,325,552,269
	Settling b	10	37		3.7	0.65	2.47	$47,000,000	$119,350,492
	Flocculation b	10	37		3.7	0.65	2.47	$1,700,000	$4,316,933
	Centrifuge b	10	37		3.7	0.65	2.47	$4,400,000	$11,173,238
	Cell rupturing b	10	37		3.7	0.65	2.47	$14,100,000	$35,805,147
	Solvent extraction b	10	37		3.7	0.65	2.47	$4,200,000	$10,665,363
	AD system c	393,100	303,617	kg/h	0.77	0.6	1	$33,782,088	$31,154,035
								Total	$1,538,017,477
Section 800 CHP									
	Recycled water pump (4X) *								$8,315,300
C801	Air compressor *								$20,408,400
GT-801	Gas turbine *								$12,631,100
ST-802	Steam Turbine *								$932,500
EX801	Heat recovery boiler								$3,383,600
C802	Biogas compressor *								$4,503,300
	Others								$929,800
								Total	$51,104,000
	Utilities incl.storage tanks etc. c								$10,220,953
								Total Capital Cost	**$1,945,286,424**

Note: * Equipment cost is estimated by Aspen Economic Analyzer; [a] Equipment cost is calculated by scaling up/down based on NETL study (base year 2007) [S4]; [b] Equipment cost is calculated by scaling up/down based on based on Davis' study (base year 2010) [S2]; [c] Equipment cost is calculated by scaling up/down based on based on Jones, *et al*.' study (base year 2007) [S1]; Please note that the pyrolysis Section 100 and the pyrolysis oil upgrading units in Section 200 have similar metrics as [S1].

Table S2. Key equipment capital cost in OP scenario

Equipment Label	Equipment Name	Original Stream Metric	New Stream Metric	Scaling Units	Size Ratio	Scaling Exp	Installed Factor	Installed Equip Cost at original Metric in base year	Installed Equip Cost at new metric in 2012$
Section 100 Pyrolysis									
	Feedstock handling [c]	2,000	2,000	tpd	1	0.7	2.47	$19,212,106	$21,687,667
R101	Pyrolyzer [c]	2,000	2,000	tpd	1	0.7	2.47	$11,699,724	$13,207,283
V102	Quench [c]	2,000	2,000	tpd	1	0.7	2.47	$6,691,470	$7,553,694
	Product recovery and storage incl. cyclone, vessel, pump and cooler [c]	2,000	2,000	tpd	1	0.7	2.47	$2,759,369	$3,114,925
	Recycle incl. sand recycle, compressor, demister [c]	2,000	2,000	tpd	1	0.7	2.47	$4,759,911	$5,373,246
								Total	$50,936,815
Section 200 Upgrading									
R201	Lipid hydrotreater *	1,959	466	scfh	0.24	0.65	2.47	$2,120,904	$940,903
R202	First stage hydrotreater [c]	1,959	1,959	scfh	1	0.65	2.47	$2,120,904	$2,394,191
R203	Second stage hydrotreater [c]	1,959	1,959	scfh	1	0.65	2.47	$22,221,810	$25,085,184
PSA-201	PSA [c]	15	15	mmscfd H2	1	0.65	2.47	$ 2,694,155	$3,041,308
E202	Heat exchanger [c]	38	38	mmbtuh	1	0.65	2.47	$1,347,791	$1,521,395
F202	Fired heater [c]	40	40	mmbtuh	1	0.65	2.47	$3,057,432	$3,451,395
C201	Hydrogen compressor [c]	2,840	2,840	acfm	1	0.65	2.47	$10,746,045	$12,130,718
	Others								$6,139,479
								Total	$54,704,573
Section 300 Separation & Section 500 Hydro cracking									
T301	Debutanizer [c]	69,495	106,548	lb/h	1.53	0.65	2.47	$222,238	$331,201
T302	Naphtha Splitter [c]	66,028	80,315	lb/h	1.22	0.65	2.47	$488,894	$626,828
T303	Diesel Splitter [c]	46,668	60,873	lb/h	1.3	0.65	2.47	$184,801	$247,945
T304	Product Splitter [c]	9,694	15,178	lb/h	1.57	0.65	2.47	$344,139	$519,917
R501	Hydrocracker Unit [c]	7,473	11,998	cuf/h	1.61	0.65	2.47	$14,130,726	$21,700,031
	Others								$2,063,291
								Total	$25,489,213

Table S2 Continued

Section 400 Carbon capture, storage and expansion									
	Absorption and desorption unit [a]	1,316,349	173,495	lb/h	0.13	0.6	2.47	$218,463,000	$72,108,068
C401a-f	CO_2 compressors *								$9,630,000
Exp401a-c	CO_2 expanders *								$1,323,000
	Others								$2,906,667
								Total	$86,967,735
Section 600 Hydrogen plant									
	Steam reformer system	3460	3797	kg/h	1.10	0.65	2.47	$ 87,152,793	$104,509,557
								Total	$104,512,765
Section 700 Microalgae cultivation and anaerobic digestion									
	Open pond system [b]	10	21	MM gallon / year	2.1	0.65	2.47	$30,000,000	$52,840,158
	Settling [b]	10	21		2.1	0.65	2.47	$47,000,000	$82,782,914
	Flocculation [b]	10	21		2.1	0.65	2.47	$1,700,000	$2,994,276
	Centrifuge [b]	10	21		2.1	0.65	2.47	$4,400,000	$7,749,890
	Cell rupturing [b]	10	21		2.1	0.65	2.47	$14,100,000	$24,834,874
	Solvent extraction [b]	10	21		2.1	0.65	2.47	$4,200,000	$7,397,622
	AD system [c]	393,100	335,390	kg/h	0.85	0.6	1	$33,782,088	$33,071,106
								Total	$211,670,840
Section 800 CHP									
	Recycled water pump (4X)*								$20,453,652
C801	Air compressor *								$9,120,000
GT-801	Gas turbine *								$6,600,000
ST-802	Steam Turbine *								$719,000
EX801	Heat recovery boiler								$4,528,400
C802	Biogas compressor *								$4,180,000
	Others								$883,000
								Total	$46,484,052
	Utilities incl.storage tanks etc. [c]								$9,789,703
								Total Capital Cost	**$590,552,508**

Note: * Equipment cost is estimated by Aspen Economic Analyzer; [a] Equipment cost is calculated by scaling up/down based on NETL study (base year 2007) [S4]; [b] Equipment cost is calculated by scaling up/down based on based on Davis' study (base year 2010) [S2]; [c] Equipment cost is calculated by scaling up/down based on based on Jones, *et al*.' study (base year 2007) [S1] ; Please note that the pyrolysis Section 100 and the pyrolysis oil upgrading units in Section 200 have similar metrics as [S1].

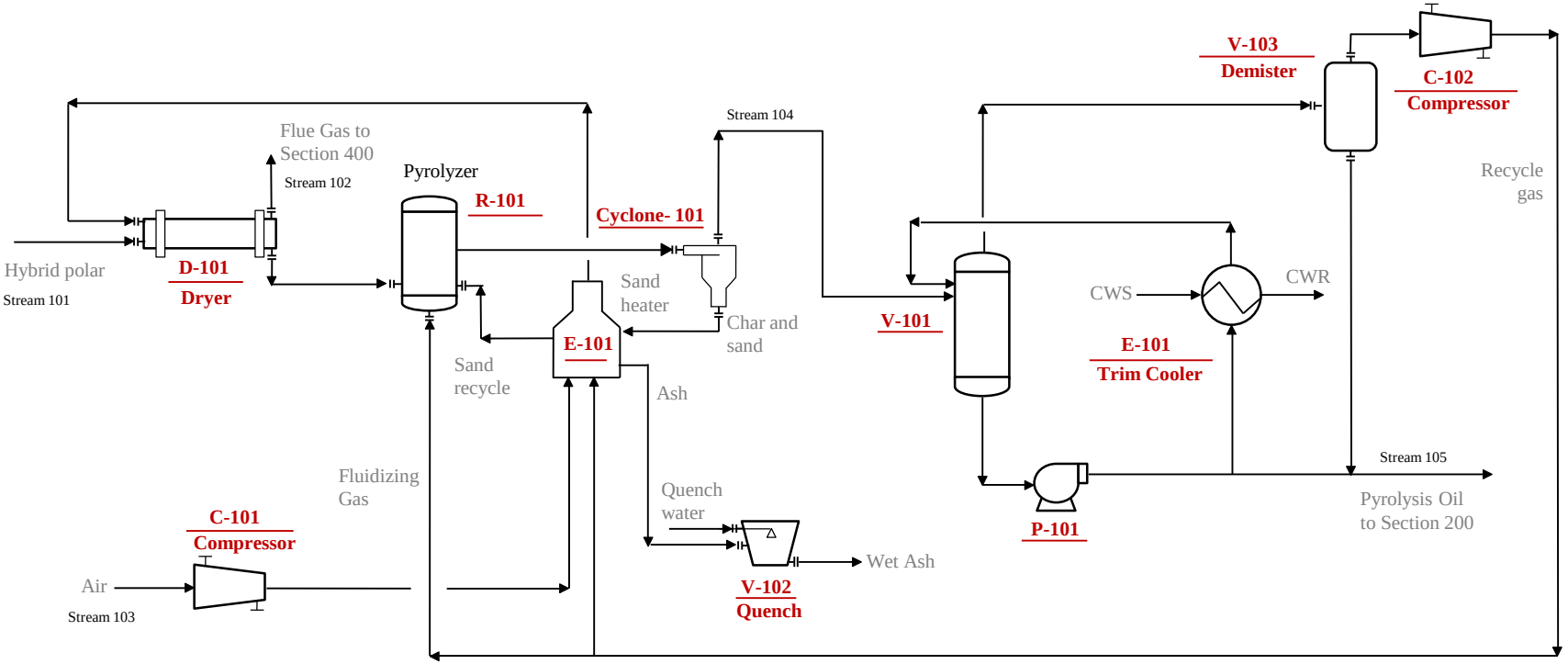

Fig. S1. Biomass Pyrolysis Section 100, adapted from Jones *et al.*, [S1].

Table S3. The flowrate and composition of main streams in Figure S1 (Pyrolysis Section)

Stream #	**101**	**102**	**103**	**104**	**105**
Operational model	Days and Nights	Days and Nights	Days and Nights	Days and Nights	Days and Nights
Flowrate (kg/h)	166666	254332	158757	162894.4449	68843.198
Temperature (K)	298.2	342.7	298.2	773.2	299.1
Pressure (bar)	1.22	1.08	1.03	1.082198	1.01
Composition (mass fraction)					
Hybrid poplar	0.5				
Oxygen		0.058	0.233		
Nitrogen		0.692	0.767	0.0300	
Water	0.5	0.026		0.0906	0.2081
Hydrogen				0.0013	
Ammonia				0.0008	
Carbon Monoxide				0.4924	
Carbon Dioxide		0.224		0.0273	0.0001
Methane				0.0025	
Ethylene				0.0098	
Propylene				0.0102	
Cellobiose				0.0637	0.1505
Levoglucosan				0.0168	0.0396
Furfural				0.0335	0.0798
HydroxyAcetone				0.0168	0.0398
Acetic Acid				0.0235	0.0540
PYLIGNIN				0.1810	0.4281

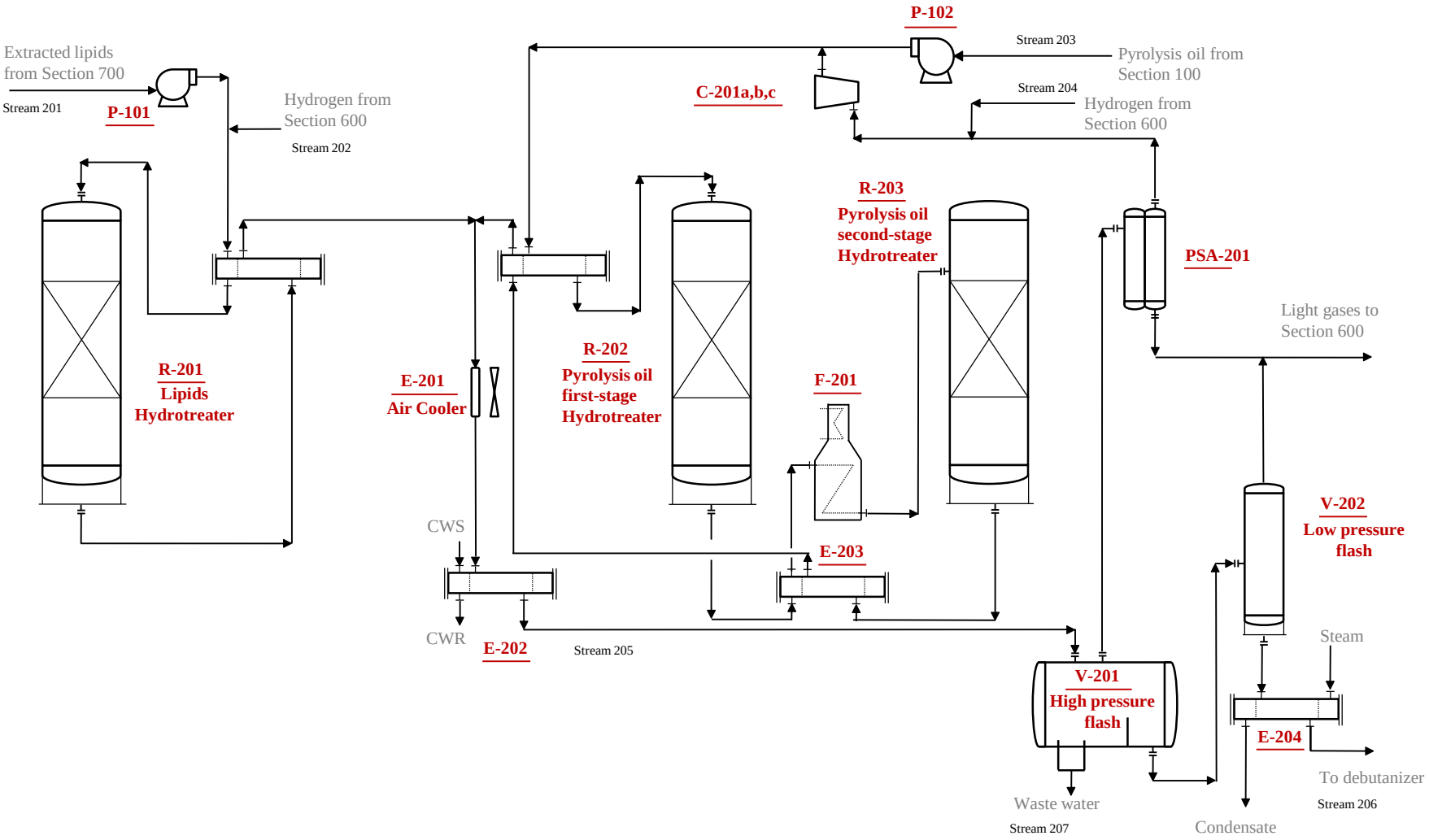

Fig. S2. Upgrading Section 200, adapted from Jones *et al.*, [S1].

Table S4.1. The flowrate and composition of main streams in Figure S2 (Upgrading Section): the photobioreactor scenario.

Stream #	**201**	**202**	**203**	**204**	**205**	**206**	**207**
Scenario	Photobioreactor	Photobioreactor	Photobioreactor	Photobioreactor	Photobioreactor	Photobioreactor	Photobioreactor
Operational period	Day and Night	Day and Night	Day and Night	Day and Night	Day and Night	Day and Night	Day and Night
Flowrate (kg/h)	13881	208	68768	2948	87475	43740	32667
Temperature (K)	298.15	298.15	316.9	298.2	316.2	366.5	310.9
Pressure (bar)	1.3	34.4737864	1.1	21.69752	49.54	42.3	49.3
Composition (mass fraction)							
Water			0.2121		0.377	0.005	0.999
Hydrogen		1		1	0.020	0.000	
Carbon Monoxide					0.001	0.000	
Carbon Dioxide					0.065	0.008	0.0007
Methane					0.017	0.000	
Ethane					0.010	0.002	
Propane					0.019	0.012	
I-Butane					0.008	0.009	
Cellobiose			0.1538				
Levoglucosan			0.0374				
Furfural			0.0767				
HydroxyAcetone			0.0399				
Acetic Acid			0.0559				
2-5-Xylenol					0.057	0.114	0.0001
N-Heptane					0.017	0.034	
1-ts-35-3C1CycC6					0.027	0.054	
3-3-5-TriMth-C7					0.011	0.022	
N-PropylCyc-C6					0.029	0.058	
1-2-3-Mesitylene					0.005	0.010	
N-ButylCycHexane					0.002	0.003	
1-2-DiC1-3C2-Bz					0.013	0.026	
Cis-Decalin					0.024	0.047	
Dimethyl-C11					0.069	0.137	
1-2-4-triethylbe					0.027	0.054	
1-1-Bicyclohexyl					0.002	0.004	
Diphenyl					0.037	0.074	
diamantane					0.073	0.145	
Phenanthrene					0.043	0.086	
N-C15-CycloC5					0.002	0.005	
CHRYSENE					0.032	0.063	
Tetralin					0.001	0.001	
P-Xylene					0.011	0.021	
C9H18					0.002	0.003	
PYLIGNIN			0.42415808				
Lipids	0.997						
Solvents	0.003						

Table S4.2. The flowrate and composition of main streams in Figure S2 (Upgrading Section): the open pond scenario.

Stream #	201	202	203	204	205	206	207
Scenario	Open Ponds	Open Ponds	Open Ponds	Open Ponds	Open Ponds	Open Ponds	Open Ponds
Operational period	Day and Night	Day and Night	Day and Night	Day and Night	Day and Night	Day and Night	Day and Night
Flowrate (kg/h)	7891	118	68768	2948	81314	38712	32575
Temperature (K)	298.2	298.2	316.9	298.2	316.2	366.5	366.5
Pressure (bar)	1.3	34.4737864	1.1	21.69752	49.54	42.3	42.3
Composition (mass fraction)							
Water		1	0.2121		0.4033	0.0053	0.9992
Hydrogen				1	0.0214		
Carbon Monoxide					0.0004		
Carbon Dioxide					0.0613	0.0080	0.0007
Methane					0.0187	0.0002	
Ethane					0.0112	0.0019	
Propane					0.0155	0.0104	
I-Butane					0.0084	0.0097	
Cellobiose			0.1538				
Levoglucosan			0.0374				
Furfural			0.0767				
HydroxyAcetone			0.0399				
Acetic Acid			0.0559				
2-5-Xylenol					0.0542	0.1138	0.0001
N-Heptane					0.0184	0.0379	
1-ts-35-3C1CycC6					0.0283	0.0592	
3-3-5-TriMth-C7					0.0115	0.0241	
N-PropylCyc-C6					0.0296	0.0619	
1-2-3-Mesitylene					0.0046	0.0097	
N-ButylCycHexane					0.0015	0.0032	
1-2-DiC1-3C2-Bz					0.0119	0.0249	
Cis-Decalin					0.0223	0.0467	
Dimethyl-C11					0.0630	0.1324	
1-2-4-triethylbe					0.0242	0.0508	
1-1-Bicyclohexyl					0.0018	0.0038	
Diphenyl					0.0334	0.0702	
diamantane					0.0655	0.1375	
Phenanthrene					0.0410	0.0861	
N-C15-CycloC5					0.0022	0.0047	
CHRYSENE					0.0341	0.0717	
Tetralin					0.0004	0.0008	
P-Xylene					0.0108	0.0225	
C9H18					0.0010	0.0022	
PYLIGNIN			0.4242				
Lipids	0.997						
Solvents	0.003						

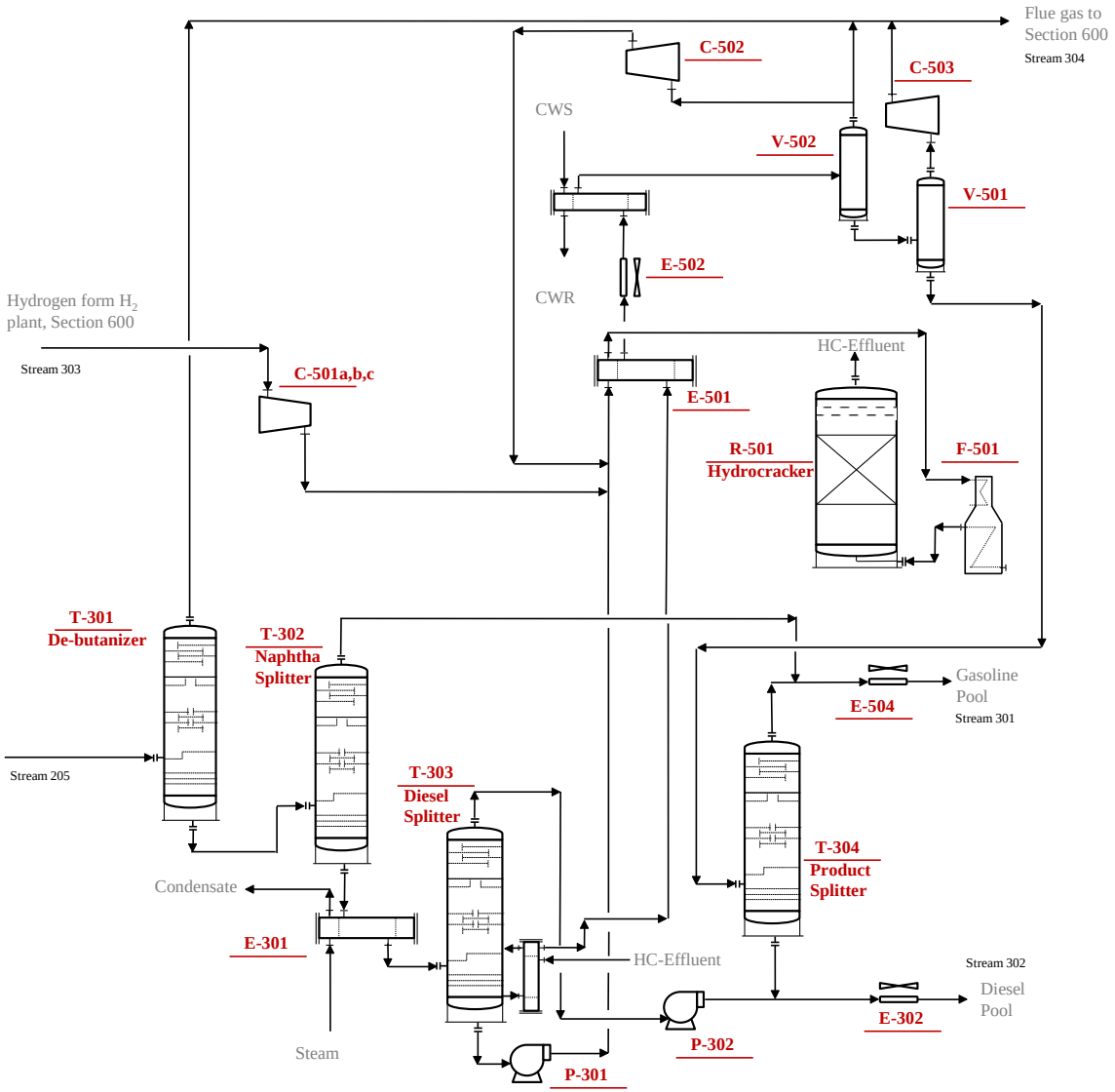

Fig. S3. Separation Section 300 and Hydrocracking Section 500, adapted from Jones, *et al.*, [S1].

Table S5.1. The flowrate and composition of main streams in Figure S3 (Hydrocracking and Separation Sections): the photobioreactor scenario.

Stream #	**301**	**302**	**303**	**304**
Scenario	Photobioreactor	Photobioreactor	Photobioreactor	Photobioreactor
Operational period	Days and Nights	Days and Nights	Days and Nights	Days and Nights
Flowrate (kg/h)	14287	27443	880	2735
Temperature (K)	416.6	433.9	298.2	310.9
Pressure (bar)	1.08	1.10	21.7	3.4
Composition (mass fraction)				
Water				0.027
Hydrogen	0.00001		1	0.021
Carbon Monoxide				0.004
Carbon Dioxide				0.438
Methane				0.116
Ethane				0.071
Propane				0.139
I-Butane				0.063
2-5-Xylenol	0.02291	0.167		
N-Heptane	0.03019			0.115
1-ts-35-3C1CycC6	0.15769	0.011		
3-3-5-TriMth-C7	0.07129	0.001		
N-PropylCyc-C6	0.16999	0.012		
1-2-3-Mesitylene	0.01948	0.007		
N-ButylCycHexane	0.00511	0.003		
1-2-DiC1-3C2-Bz	0.01260	0.035		
Cis-Decalin	0.01550	0.067		
Dimethyl-C11	0.00298	0.214		
1-2-4-triethylbe	0.00005	0.084		
1-1-Bicyclohexyl		0.006		
Diphenyl		0.116		
diamantane		0.227		
Phenanthrene		0.005		
N-C15-CycloC5		0.001		
Cyclopentane	0.00004			
Tetralin	0.00042	0.007		
N-Butane	0.00354			0.001
P-Xylene	0.07194			
C9H18	0.27998	0.038		
MthCyclohexane	0.13627			0.003

Table S5.2. The flowrate and composition of main streams in Figure S3 (Hydrocracking and Separation Sections): the open pond scenario.

Stream #	**301**	**302**	**303**	**304**
Scenario	Open Ponds	Open Ponds	Open Ponds	Open Ponds
Operational period	Days and Nights	Days and Nights	Days and Nights	Days and Nights
Flowrate (kg/h)	13077.47	23625.82	730	2325.77
Temperature (K)	416.567909	433.894657	298.15	310.94006
Pressure (bar)	1.08	1.1	21.69752188	3.42
Composition (mass fraction)				
Water				0.027
Hydrogen			1	0.023
Carbon Monoxide				0.003
Carbon Dioxide				0.432
Methane				0.130
Ethane				0.080
Propane				0.120
I-Butane				0.070
2-5-Xylenol	0.0347	0.1672		0.000
N-Heptane	0.0433			0.108
1-ts-35-3C1CycC6	0.1752			0.001
3-3-5-TriMth-C7	0.0715			0.000
N-PropylCyc-C6	0.1833			0.001
1-2-3-Mesitylene	0.0285	0.0002		
N-ButylCycHexane	0.0091	0.0002		
1-2-DiC1-3C2-Bz	0.0239	0.0276		
Cis-Decalin	0.0247	0.0629		
Dimethyl-C11	0.0061	0.2133		
1-2-4-triethylbe		0.0830		
1-1-Bicyclohexyl		0.0059		
Diphenyl		0.0911		
diamantane		0.1635		
Phenanthrene		0.0002		
N-Pentadecane		0.0001		
N-Octadecane				
Tetralin		0.0087		
N-Butane	0.0047			0.002
P-Xylene	0.0667			0.000
C9H18	0.1493	0.1761		0.001
MthCyclohexane	0.1787			0.003

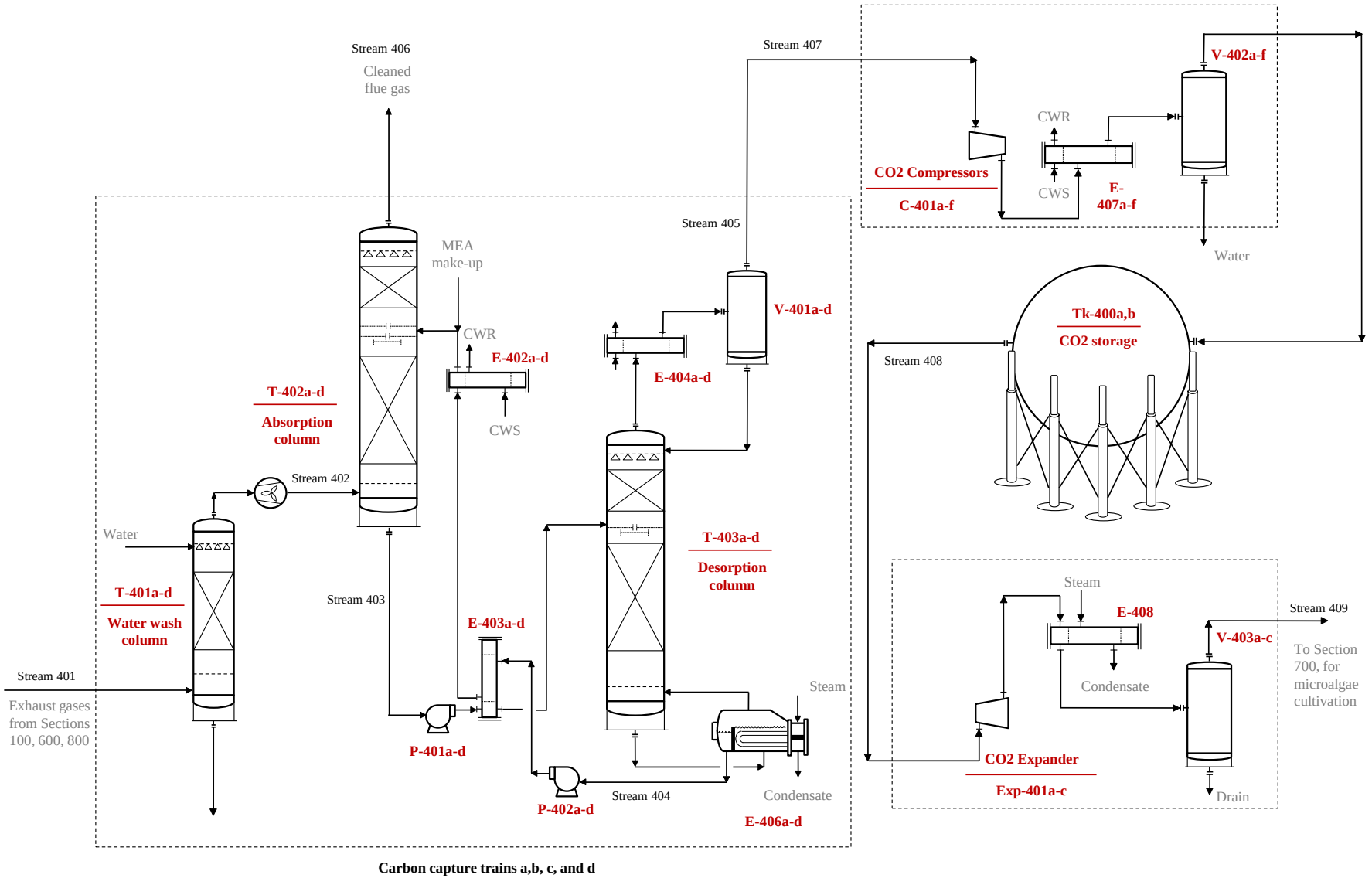

Fig. S4. Carbon Capture, storage and expansion, Section 400

Table S6.1. The flowrate and composition of main streams in Figure S4 (Carbon Capture, storage and expansion): the photobioreactor scenario.

Stream #	**401**	**402**	**403**	**404**	**405**	**406**	**407**	**408**	**409**
Scenario	Photobioreactor	Photobioreactor	Photobioreactor	Photobioreactor	Photobioreactor	Photobioreactor	Photobioreactor	Photobioreactor	Photobioreactor
Operational period	Nights	Nights	Nights	Nights	Nights	Nights	Nights	Days	Days
Flowrate (kg/h)	733973	155074	995760	972000	28809	530496	115235	115235	115235
Temperature (K)	408.2	316.8	332.5	388.4	314.0	320.4	314.0	308.15	308.15
Pressure (bar)	1.2	1.3	1.1	1.86	1.82	1.14	1.82	153	2
Composition (mass fraction)									
CO2	0.175	0.206	0.094	0.068	0.982	0.0228	0.982	0.999	0.999
Water	0.165	0.017	0.631	0.650	0.018	0.0675	0.018	0.001	0.001
O2	0.052	0.062				0.0721			
N2	0.605	0.715				0.8379			
MEA			0.275	0.282					

Table S6.2. The flowrate and composition of main streams in Figure S4 (Carbon Capture, storage and expansion): the open pond scenario.

Stream #	**401**	**402**	**403**	**404**	**405**	**406**	**407**	**408**	**409**
Scenario	Open Ponds	Open Ponds	Open Ponds	Open Ponds	Open Ponds	Open Ponds	Open Ponds	Open Ponds	Open Ponds
Operational period	Nights	Nights	Nights	Nights	Nights	Nights	Nights	Days	Days
Flowrate (kg/h)	485085	98964	686160	666360	19674	330048	78696	78696	78696
Temperature (K)	408.2	316.8	332.5	388.4	314.0	320.4	314.0	308.15	308.15
Pressure (bar)	1.2	1.3	1.1	1.9	1.8	1.1	1.8	153.0	2.0
Composition (mass fraction)									
CO2	0.179	0.218	0.094	0.068	0.982	0.028	0.982	0.999	0.999
Water	0.165	0.031	0.631	0.649	0.018	0.071	0.018	0.001	0.001
O2	0.051	0.059				0.071			
N2	0.605	0.693				0.830			
MEA			0.275	0.283					

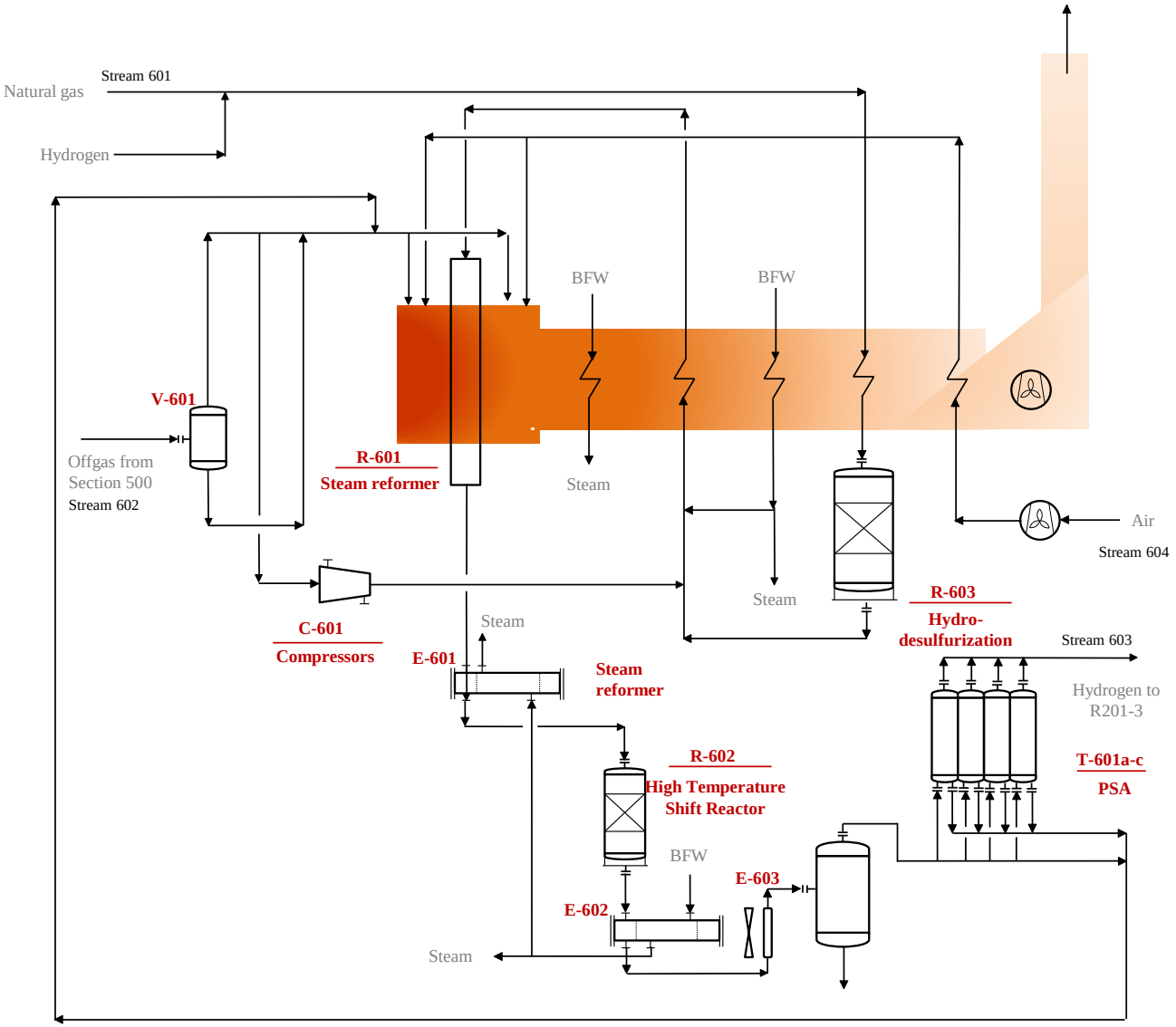

Fig. S5. Hydrogen production Section 600- adapted from Jones *et al.*, [S1].

Table S7.1. The flowrate and composition of main streams in Figure S5 (Hydrogen production Section): the photobioreactor scenario.

Stream #	**601**	**602**	**603**	**604**
Scenario	Photobioreactor	Photobioreactor	Photobioreactor	Photobioreactor
Operational period	Days and Nights	Days and Nights	Days and Nights	Days and Nights
Flowrate (kg/h)	7600	9560.75	3895.9	145000
Temperature (K)	298.15	310.94006		298.15
Pressure (bar)	28.6	3.42		1.1
Composition (mass fraction)				
Water		0.027		
Hydrogen		0.021	1	
Carbon Monoxide		0.004		
Carbon Dioxide		0.438		
Methane	1	0.116		
Ethane		0.071		
Propane		0.139		
I-Butane		0.063		
N-Heptane		0.115		
N-Butane		0.001		
MthCyclohexane		0.003		
O2				0.232
N2				0.768

Table S7.2. The flowrate and composition of main streams in Figure S5 (Hydrogen production Section): the open pond scenario.

Stream #	**601**	**602**	**603**	**604**
Scenario	Open Ponds	Open Ponds	Open Ponds	Open Ponds
Operational period	Days and Nights	Days and Nights	Days and Nights	Days and Nights
Flowrate (kg/h)	7550	8540.77	3796.7111	140000
Temperature (K)	298.15	310.94006		298.15
Pressure (bar)	28.6	3.42		1.1
Composition (mass fraction)				
Water		0.027		
Hydrogen		0.023	1	
Carbon Monoxide		0.003		
Carbon Dioxide		0.432		
Methane	1	0.130		
Ethane		0.080		
Propane		0.120		
I-Butane		0.070		
N-Heptane		0.108		
C9H18		0.001		
MthCyclohexane		0.003		
O2				0.232
N2				0.768

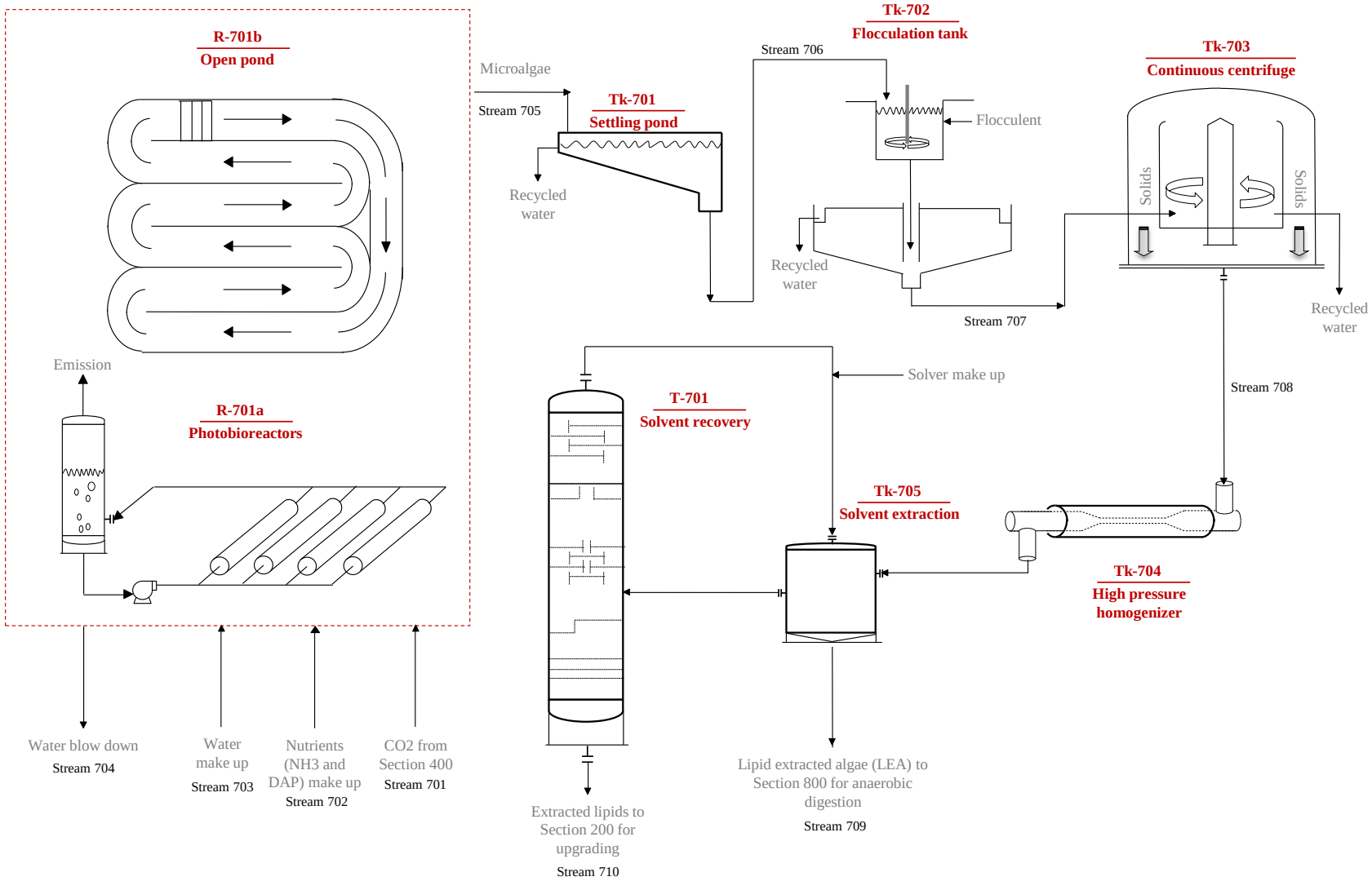

Fig. S6. Microalgae cultivation, Section 700

Table S8.1. The flowrate and composition of main streams in Figure S6 (Microalgae Cultivation Section): the photobioreactor scenario.

Stream #	**701**	**702**	**703**	**704**	**705**	**706**	**707**	**708**	**709**	**710**
Operational mode	Photobioreactor	Photobioreactor	Photobioreactor	Photobioreactor	Photobioreactor	Photobioreactor	Photobioreactor	Photobioreactor	Photobioreactor	Photobioreactor
Operational period	Days	Days	Days	Days	Days	Days	Days	Days	Days	Days
Flowrate (kg/h)	230470.4301	17456.93	1545820	1545820	31550400	12695800	1382920	633995	607233	27762.28
Temperature (K)	298.15	298.15	298.15	298.15	298.15	298.15	298.15	298.15	445.9	298.15
Pressure (bar)	1.3	1.3	1.3	1.3	1.3	1.3	1.3	1.3	1.3	1.3
Composition (mass fraction)										
CO2	1									
Water			1	1	0.996	0.990	0.909	0.801	0.837	
Diammonium phosphate (DAP)		0.37								
Ammonia		0.63								
Lipids					0.001	0.0025	0.023	0.050	0.008	0.997
Proteins					0.001	0.0025	0.023	0.050	0.052	
Carbohydrates					0.002	0.0050	0.046	0.099	0.104	
Butanol (solvent)										0.003

Table S8.2. The flowrate and composition of main streams in Figure S6 (Microalgae Cultivation Section): the open pond scenario.

Stream #	**701**	**702**	**703**	**704**	**705**	**706**	**707**	**708**	**709**	**710**
Operational mode	Open Ponds	Open Ponds	Open Ponds	Open Ponds	Open Ponds	Open Ponds	Open Ponds	Open Ponds	Open Ponds	Open Ponds
Operational period	Days	Days	Days	Days	Days	Days	Days	Days	Days	Days
Flowrate (kg/h)	155814.2214	11803.01	6928650	6928650	138923000	7012170	763821	350172	335390	15781.48
Temperature (K)	298.15	298.15	298.15	298.15	298.15	298.15	298.15	298.15	298.15	445.9
Pressure (bar)	1.3	1.3	1.3	1.3	1.3	1.3	1.3	1.3	1.3	1.3
Composition (mass fraction)										
CO2	1									
Water			1	1	0.9995	0.9901	0.9089	0.8014	0.8367	
Diammonium phosphate (DAP)		0.37								
Ammonia		0.63								
Lipids					0.0001	0.0025	0.0228	0.0497	0.0078	0.997
Proteins					0.0001	0.0025	0.0228	0.0497	0.0518	
Carbohydrates					0.0003	0.0050	0.0455	0.0993	0.1037	
Butanol (solvent)										0.003

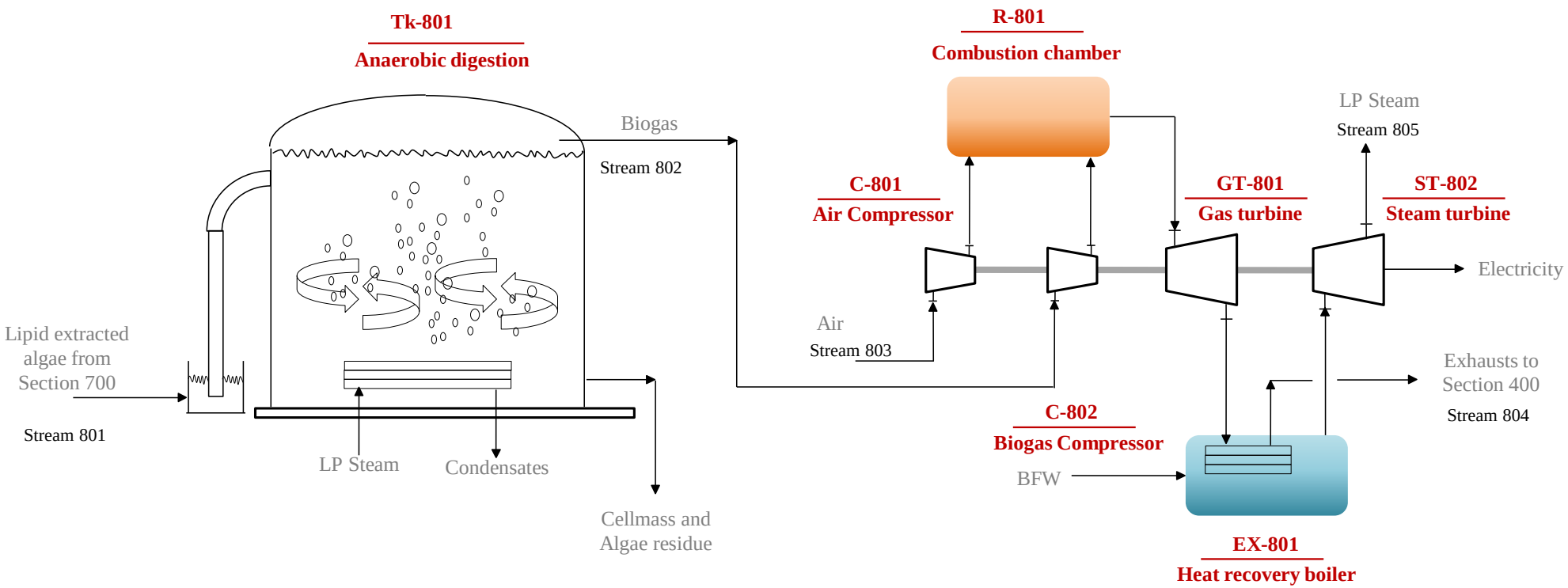

Fig. S7. Anaerobic Digestion Section and combined heat and power (CHP) cycle, Section 800

Table S9.1. The flowrate and composition of main streams in Figure S7 (Anaerobic Digestion and CHP Sections): the photobioreactor scenario.

Stream #	**801**	**802**	**803**	**804**	**805**
Operational mode	Photobioreactor	Photobioreactor	Photobioreactor	Photobioreactor	Photobioreactor
Operational period	Day and Night	Day and Night	Day and Night	Day and Night	Day and Night
Flowrate (kg/h)	303617	24498.53	275000	295132	40000
Temperature (K)	298.2	298.2	298.2	408.2	406.7
Pressure (bar)	1.3	1.3	1.3	1.1	3
Composition (mass fraction)					
CO2		0.552		0.145	
Water	0.837	0.014	0.018	0.085	1.000
Methane		0.434			
DIAMPHOS					
AMMONIA					
Lipids	0.008				
Proteins	0.052				
Carbohydrates	0.104				
O2			0.229	0.069	
N2			0.753	0.702	

Table S9.2. The flowrate and composition of main streams in Figure S7 (Anaerobic Digestion and CHP Sections): the open pond scenario.

Stream #	**801**	**802**	**803**	**804**	**805**
Operational mode	Open Ponds	Open Ponds	Open Ponds	Open Ponds	Open Ponds
Operational period	Day and Night	Day and Night	Day and Night	Day and Night	Day and Night
Flowrate (kg/h)	167695	13487.17	110000	121683	30000
Temperature (K)	298.2	298.2	298.2	408.2	406.7
Pressure (bar)	1.3	1.3	1.3	1.1	3
Composition (mass fraction)					
CO2		0.550		0.150	
Water	0.837	0.015	0.018	0.088	1
Methane		0.435			
DIAMPHOS					
AMMONIA	0.008				
Lipids	0.052				
Proteins	0.104				
Carbohydrates					
O2			0.229	0.063	
N2			0.753	0.699	